Thesis, COLLÉGIALITÉ

Auteur : Spahic, Enes
Promoteur(s) : Delacroix, Laurence; Malgrange, Brigitte
Faculté : Faculté de Médecine
Diplôme : Master en sciences biomédicales, à finalité approfondie
Année académique : 2023-2024
URI/URL : http://hdl.handle.net/2268.2/20550

LIÈGE université
Médecine

LIÈGE université
GIGA
Neurosciences

Role of the Extracellular matrix in Hearing

Academic year 2023 – 2024
Developmental neurobiology unit, GIGA Stem cells

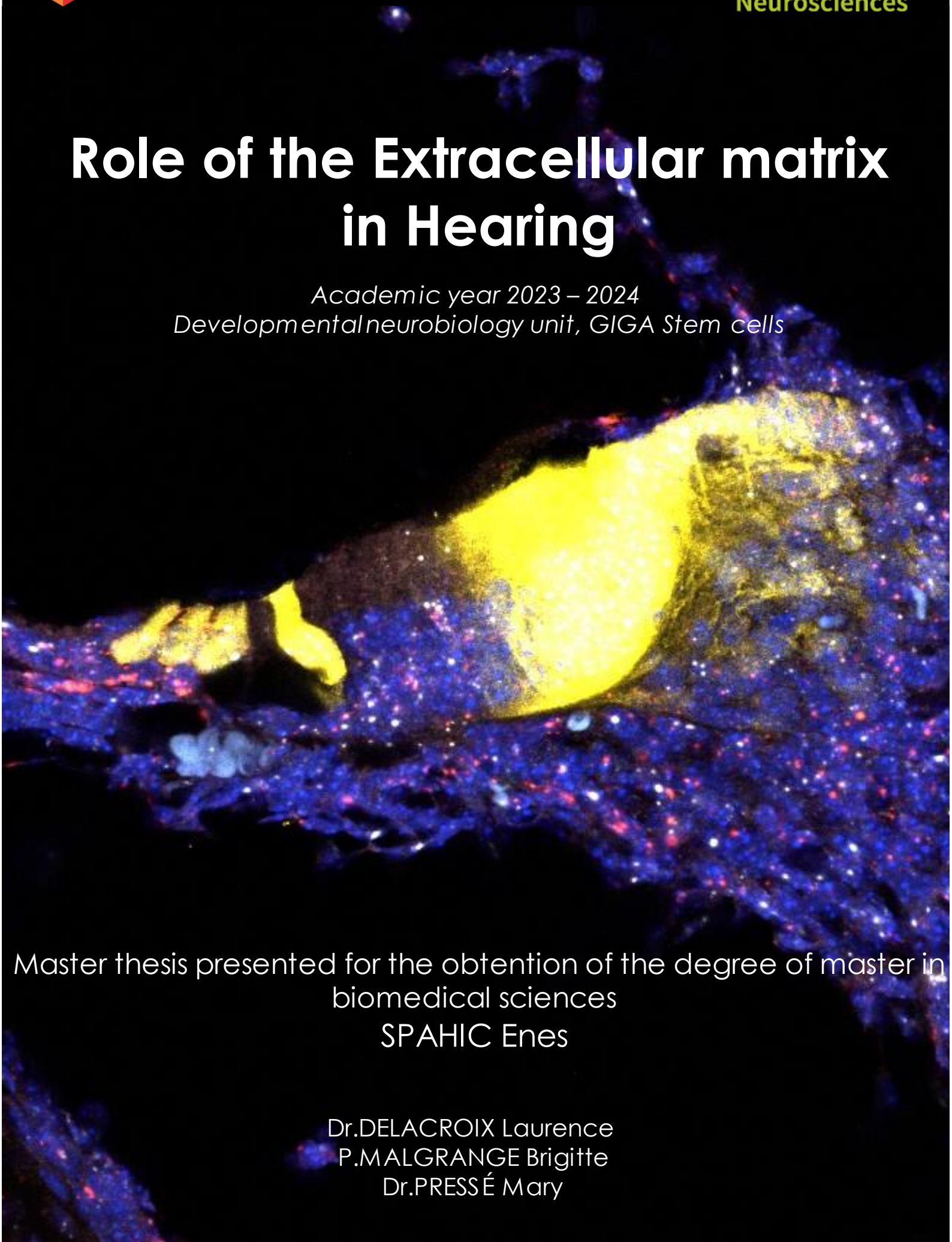

Master thesis presented for the obtention of the degree of master in biomedical sciences

SPAHIC Enes

Dr.DELACROIX Laurence
P.MALGRANGE Brigitte
Dr.PRESSÉ Mary

Abstract

Mutations in extracellular matrix (ECM) related genes have been increasingly associated with hearing impairments in humans. By providing viscoelastic properties to the resonant structures of the inner ear, mechanical and trophic support to the cells and participating in cell signalling in response to environmental changes, the ECM is crucial for hearing function. In this work, we investigated some of its critical regulators namely, Cemip hyaluronidase, and the matrix metalloproteinases, MMP2 and MMP9.

By using a mouse model invalidated for Cemip, we studied the hearing function at different ages to analyse whether hyaluronic acid (HA) accumulation could impair audition. Results from auditory brainstem recordings (ABR) reveal no obvious hearing decline in Cemip-deficient mice, up to 16 weeks of age. Future functional studies, up to 1 year of age, will allow us to know if age-related hearing loss may be accelerated or exacerbated in the absence of Cemip. However, we can conclude that Cemip, which is defined as a deafness-causing gene in humans, is not essential for hearing in young adult mice.

As noise overexposure has been reported to trigger ECM breakdown and remodelling, we characterized MMP2 and MMP9 gelatinases expression and localisation changes in a noise-induced hearing loss mouse model. At the level of the whole cochlea, MMP2 transcript level tended to increase from 2 hours to 3 days following noise exposure, while MMP9 transcript tended to decrease progressively from 1 day to 7 days after trauma. Immunostainings revealed that MMP2 protein was upregulated throughout the cochlear tissue as soon as 2 hours following noise, particularly in the surrounding bony capsule but also at the level of the spiral ligament and auditory nerve fibres. In contrast, noise only induced a local accumulation of MMP9 in the spiral ligament. Altogether, our results suggest that MMP2 and MMP9 might be involved in local ECM remodelling after noise exposure, however, further studies are required to verify whether their presence translates into gelatinase activity.

Résumé

Les mutations dans les gènes liés à la matrice extracellulaire (MEC) ont été associés de plus en plus avec des défauts auditifs chez l'homme. En conférant les propriétés viscoélastiques aux structures résonantes de l'oreille interne, un support mécanique et trophique aux cellules et en participant à la signalisation cellulaire en réponse à des changements environnementaux, la MEC est cruciale pour la fonction auditive. Dans ce projet, nous avons investigué certains de ces régulateurs les plus importants notamment, la hyaluronidase Cemip ainsi que les métalloprotéinase matricielles, MMP2 et MMP9.

Au moyen d'un modèle murin délété du gène Cemip, nous avons étudies la fonction auditive à différents âges afin d'analyser si l'accumulation d'acide hyaluronique (HA) pouvait détériorer l'audition. Des résultats de potentiels évoqués auditifs (PEA) ne démontrent pas de déclin évident dans l'audition de souris Cemip-déficiente jusqu'à 16 semaines. De futures études fonctionnelles, jusqu'à 1 an d'âge, nous permettront de savoir si la perte auditive liée à l'âge peut être accélérée ou exacerbée en l'absence de Cemip. Toutefois, nous pouvons conclure que Cemip, un gène responsable de surdités chez l'Homme, n'est pas essentiel à l'audition chez les jeunes souris adultes.

Etant donné qu'il a été montré que l'exposition sonore provoque une dégradation et un remodelage de la MEC, nous avons caractérisé l'expression des gélatinases MMP2 et MMP9 ainsi que leurs changements de localisation dans un modèle murin d'exposition sonore. Au niveau de la cochlée entière, le niveau de transcrit de MMP2 tendait à augmenter de 2h à 3 jours suivant l'exposition alors que le niveau de transcrit de MMP9 tendant à décroitre progressivement du jour 1 au jour 7. Les immunomarquages ont quant à eux révélé que la protéine MMP2 était augmentée dans le tissu cochléaire aussitôt que 2h suivant l'exposition sonore, particulièrement dans la capsule osseuse mais aussi au niveau du ligament spiral et des fibres nerveuses auditives. Parallèlement, l'exposition au bruit a induit une accumulation de MMP9 au niveau du ligament spiral. Somme toute, nos résultats suggèrent que MMP2 et MMP9 pourraient être impliqués dans le remodelage local de la MEC après l'exposition sonore, cependant, des études supplémentaires doivent être menées afin de vérifier si leur présence traduit leur activité.

Acknowledgements

J'aimerais tout d'abord remercier le Pr. Brigitte Malgrange de m'avoir permis de réaliser mon mémoire au sein de son laboratoire, imbibé par la passion scientifique qu'on y voue à l'oreille.

J'aimerais également remercier le Dr. Laurence Delacroix pour l'incommensurabilité du temps et de la disponibilité qu'elle m'a consacré, sans jamais perdre de sa joie ni de sa hargne scientifique contagieuse. Cette expérience n'aurait pu être la même sans toi.

Je ressens une immense gratitude envers (le maintenant docteur) Mary, pour ta grande patience et ton soutien indéfectible, de près ou de loin. Je pense que j'ai pu trouver plus qu'un superviseur génial en toi, j'y ai également trouvé une source d'inspiration et une amie toujours à l'écoute. Je suis extrêmement heureux et reconnaissant d'avoir pu partager un bout de chemin avec toi.

Un très grand merci à Valentin pour m'avoir pris sous son aile dès mon arrivée au laboratoire, j'en ai appris énormément à tes côtés et je suis reconnaissant du point auquel tu t'es mobilisé pour ma réussite, souvent avec sagesse, toujours avec humour.

Je me dois également de remercier toutes les personnes sur qui j'ai pu compter au labo et sans qui je n'aurais certainement pas pu mener à bien mon projet, notamment Sali, Mona, PB, Camille, Axel et -comment l'oublier- Auriane. Sans votre aide et vos précieux conseils, je n'aurais certainement pas pu mener à bien mon projet.

Je remercie également mes co-mémorants du GIGA neuro, Chloé, Tatiana et Thomas. Notre petit groupe a beaucoup égayé mon passage au GIGA neuro et cette expérience n'aurait certainement pas été si plaisante sans vous.

Enfin, j'aimerais remercier ma famille ainsi que tous les amis avec qui j'ai partagé ou non ces années d'étude. Je ressens une gratitude ineffable envers Sibel et Katia, mes besties for ever, pour leur présence et leurs -nombreux- encouragements, lesquels m'ont permis de croire en moi et en mon accomplissement.

Table of Contents

Abbreviations

ABR	Auditory brainstem response
ARHL	Age-related hearing loss
BM	Basilar membrane
Cemip	Cell Migration Inducing hyaluronidase 1, KIAA1199
ECM	Extracellular matrix
GAG	Glycosaminoglycan
GWAS	Genome-wide genetic association studies
HA	Hyaluronic acid, hyaluronan
HABP	Hyaluronic acid binding protein
HAS	Hyaluronan synthase
HC	Hair cell
HMW-HA	High molecular weight hyaluronic acid
Hyal	Hyaluronidase or hyaluronoglucosaminidase
IHC	Inner hair cell
LMW-HA	Low molecular weight hyaluronic acid
MET	Mechanoelectrical transduction
MMP	Matrix MetalloProteinase
MMW-HA	Medium molecular weight hyaluronic acid
NIHL	Noise-induced hearing loss
OHC	Outer hair cell
PG	Proteoglycan
PNN	Perineuronal net
ROS	Reactive oxygen species
SGN	Spiral ganglion neuron
SL	Spiral limbus
S lig	Spiral ligament
SV	Stria vascularis
TM	Tectorial membran

Introduction

According to the World Health Organization, 5% of the world's population, corresponding to 430 million people, currently suffer from hearing loss. By 2050, it is expected that one out of ten people will suffer from a disabling hearing loss.

Hearing loss can be of genetic origin or of acquired origin, which relates to ototoxic drugs, noise exposure or aging. Currently, there is no treatment able to restore hearing as the vulnerable cells that are affected in the inner ear are not able to regenerate. The only clinical management available rely on devices destined to compensate for hearing loss, such as hearing aids and cochlear implants. Hence, it is important to identify the key factors affecting cochlear development, maturation, and maintenance to give rise to new therapeutical perspectives.

As there are currently no therapies that allow hair cell regeneration, new therapeutical interventions that prevent hair cell degeneration or allow for the replacement of lost hair cells are being investigated.

Hence, it is crucial we gather knowledge about the inner ear as to understand the molecular mechanisms underlying hair cell homeostasis and hearing function. This way, new targeted therapies could be discovered and potentially treat the millions of patients suffering from hearing loss currently.

1. Ear Anatomy and Function

The ear is composed of three different regions commonly referred to as the outer, middle, and inner ear (Figure 1). The outer ear is composed of the auricle and the ear canal, while the middle ear comprises the tympanic membrane and the associated bone chain formed by the Malleus, incus, and Stapes (Heine 2004). The inner ear contains the vestibule, responsible for balance, and the cochlea, responsible for hearing. The main role of the external and middle ear is to capture and amplify sound waves before they reach the cochlea, where sound decoding and hearing perception take place. When sound penetrates the ear canal, it travels to the tympanic membrane which vibrates. This vibration is then transmitted to the cochlea through the bone chain of the middle ear (Milenkovic et al. 2020). Accordingly, hearing impairments that are caused by defects in the external or middle ear are qualified as conductive hearing loss, whereas abnormalities within the inner ear are qualified as sensorineural hearing loss (Shave, Botti, and Kwong 2022).

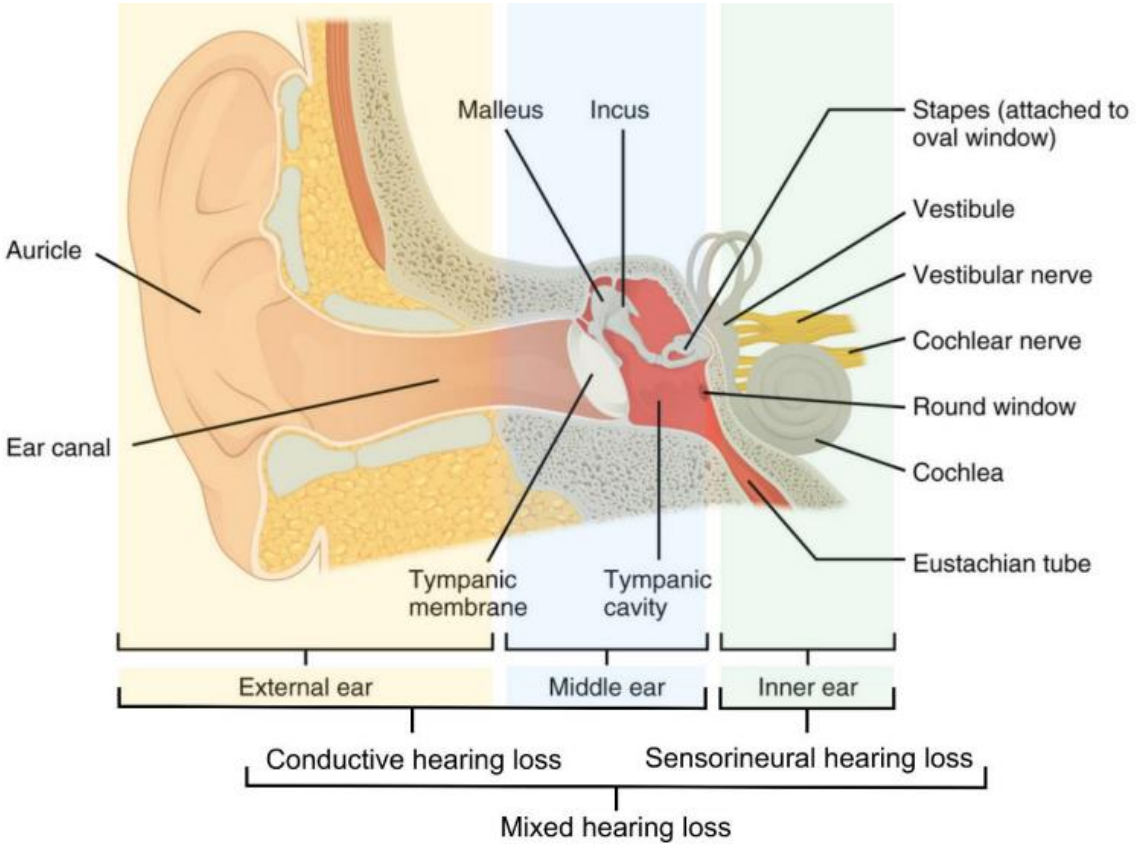

Figure 1: Inner ear anatomy

The ear comprises three distinct regions. The outer ear comprises the auricle and ear canal and stops at the tympanic membrane. The middle ear contains the three ossicles while the inner ear contains the vestibule, responsible for balance, and the cochlea, responsible for hearing. Adapted from usherkidsuk.com

1.1. The Cochlea

As the main organ of hearing, the cochlea adopts a spiral-like shape and is composed of three ramps wrapped around a bony structure called modiolus (Figure 2). Two of these ramps, called the scala vestibuli, or vestibular ramp, and scala tympani, or tympanic ramp, are filled with perilymph, a biological fluid whose composition is similar to plasma or cerebrospinal fluid (high Na^+ and low K^+ and Ca^{2+} concentrations) (Jean et al. 2023). In contrast, the central ramp, called the scala media, or cochlear duct, is filled with a potassium enriched fluid called the endolymph, crucial to hearing function. The cochlear duct is limited by the lateral wall and the basilar membrane (BM) ventrally (K. X. Kim et al. 2014). The sound waves that hit the cochlea induce a pressure change in the endolymph, causing the BM, which is the resonant structure of the cochlea, to vibrate.

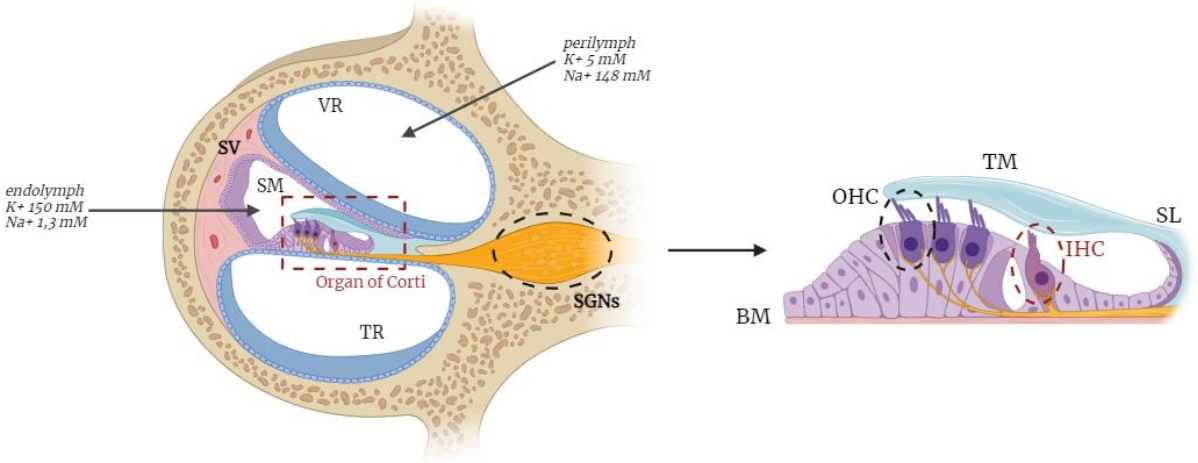

Figure 2: Cross section of the cochlea (left) and the organ of Corti (right).

Two ramps, the vestibular ramps (VR) and tympanic ramps (TR), are filled with perilymph, containing 5 mM of K^+ and 148 mM of Na^+. The scala media (SM) is filled with endolymph composed of 150 mM of K^+ and 1,3 mM of Na^+ (left). This central ramp houses the organ of Corti that comprises 3 rows of outer hair cells (OHCs) and one row of inner hair cells (IHCs), and which is flanked by membranes, namely the tectorial membrane (TM), the basilar membrane (BM) and the spiral limbus (SL) (right).

The distinctive shape of the cochlea is linked to its tonotopy, which allows for different sound frequencies to be perceived at different portions of this spiral (Figure 3). Indeed, the sound-induced wave travels along the longitudinal axis of the BM, allowing for different sound frequencies to be decoded by different regions of the cochlea. As such, low sound frequencies

are detected at the apex, while high sound frequencies are detected at the base of the spiral (Fettiplace 2023).

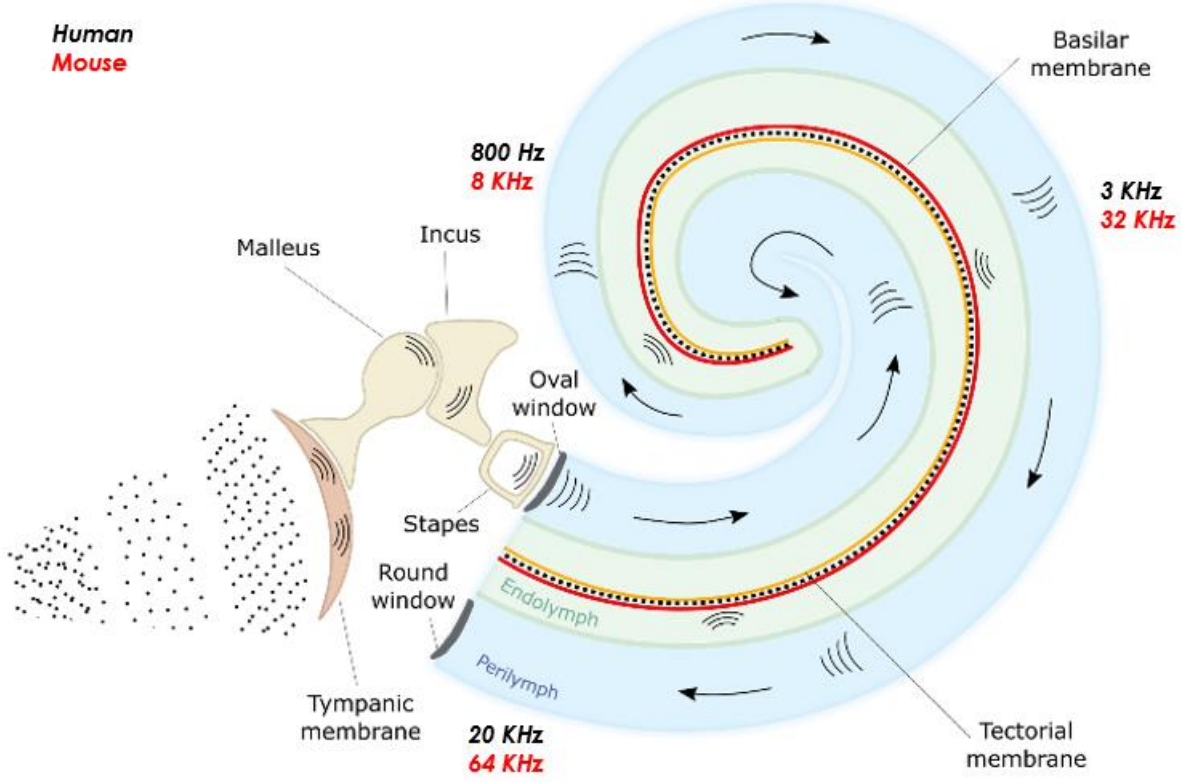

Figure 3: Longitudinal section of the cochlea.

Tonotopy is represented for human (black) and mouse (red) sound frequencies and the different regions at which they are perceived. Higher frequencies are perceived at the basal region of the cochlea whereas lower frequencies are perceived at the apical region of the cochlea. Adapted from Pressé, Malgrange, Delacroix 2024.

1.2. The Organ of Corti

The Organ of Corti lies on the basilar membrane (Figure 2), inside the scala media and is connected apically to the Tectorial membrane (TM), an acellular gel-like structure that floats in the endolymph (Goodyear et al. 2017). This organ is the sensory epithelium responsible for hearing and more precisely, for the conversion of mechanical sound waves into electrical impulses. It is rigorously organised as a checkerboard-like mosaic of sensory cells, the hair cells (HCs), and their supporting cells (SCs) (Xie et al. 2023). The organ of hearing is connected to the peripheral projections of spiral ganglion neurons (SGNs), which constitute the first relay of the hearing pathway, allowing for the transmission of the signal to the central nervous system (Zhang et al. 2013).

A. Hair cells

Hair cells are sensory cells able to detect sound-induced vibrations and transmit signals to the auditory neurons of the spiral ganglion (Figure 4). At their apical pole lie actin-based protrusions called stereocilia, organised in a V-like shape, which deflect upon the displacement of the tectorial and basilar membranes (Landin Malt et al. 2019). This deflection allows mechanoelectrical transduction channels (MET-channels), which lie at the tips of the stereocilia, to open and trigger hair cell activation (Caprara and Peng 2022). As these channels are mechanically-gated potassium channels, K^+ enters the hair cells and depolarizes them, triggering the opening of voltage-gated calcium channels (Ren, He, and Kemp 2016). Glutamate is then released by the hair cells into the synaptic cleft, leading to activation of the spiral ganglion neurons. This explains why high K^+ concentration inside the endolymph is crucial to the hearing function.

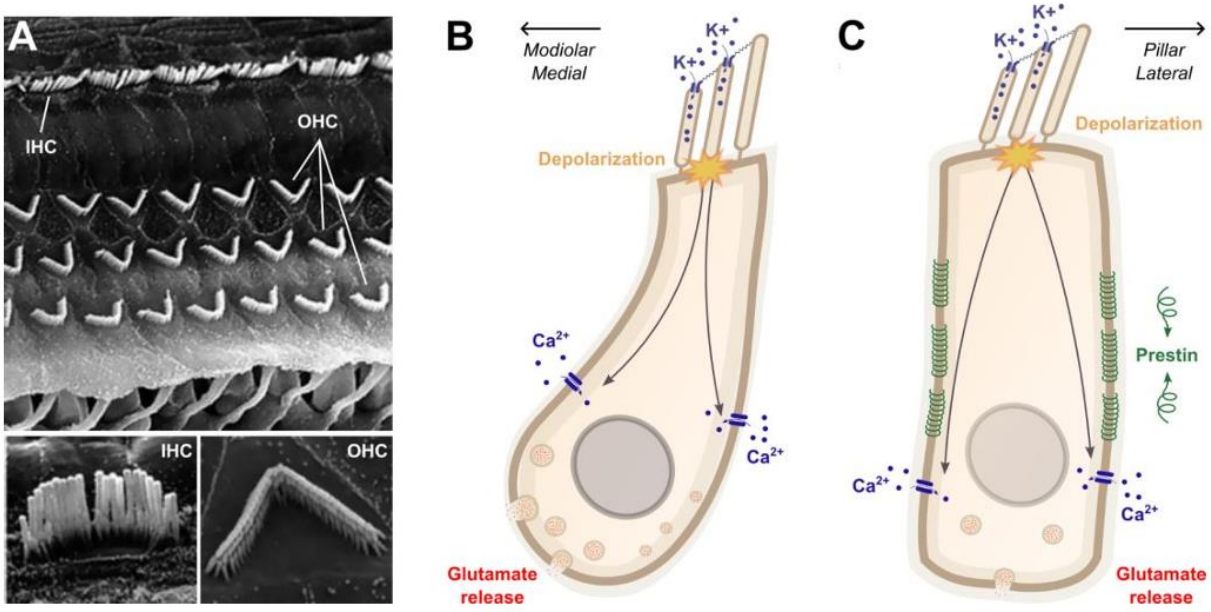

Figure 4: Inner and outer hair cell organisation and hair bundle.

A. Top view of the hair cells where apical stereocilia can be seen forming a V-shape, with cells attaining a diameter of about 6 µm. **B.** Depolarization of IHCs through the MET channels and glutamate release. **C.** Contraction of OHCs thanks to the electromotility protein prestin.

Two subtypes of sensory cells exist in the Organ of Corti, namely the outer hair cells (OHCs) and inner hair cells (IHCs). At the anatomical level, these cells are organised in one unique row of IHCs followed by three parallel rows of OHCs (Cohen and Sprinzak 2021). While IHCs specialise in sound detection, OHCs are contractile cells whose main function is cochlear amplification (Figure 4). This process refers to the amplification of the vibrations of the cochlear membranes

flanking the organ of Corti thanks to the electromotility properties of OHCs (Zheng et al. 2000). This is due to the presence of Prestin in the lateral membrane of the cells, a motor protein that is able to contract upon membrane depolarization.

B. Supporting cells

Within the organ of Corti, the hair cells are surrounded by the supporting cells, essential for the sensory epithelium structure and function (Figure 5). Unlike HCs, they span the entire depth of the organ of Corti, and possess a rigid cytoskeleton, crucial for structural integrity (Wan, Corfas, and Stone 2013). They are connected to neighbouring cells by tight and adherens junctions, sealing off the epithelium and preventing fluid leakage but are also connected to other supporting cells by tight junctions, enabling ion recycling. Besides these common features, they have distinct morphological characteristics and specific roles according to their location in the organ of Corti. Amongst them are Deiter's cells, Hensen's cells, pillar cells and many others. Interestingly, these cells have also been shown to be able to transdifferentiate into hair cells (H.-B. Zhao et al. 2006).

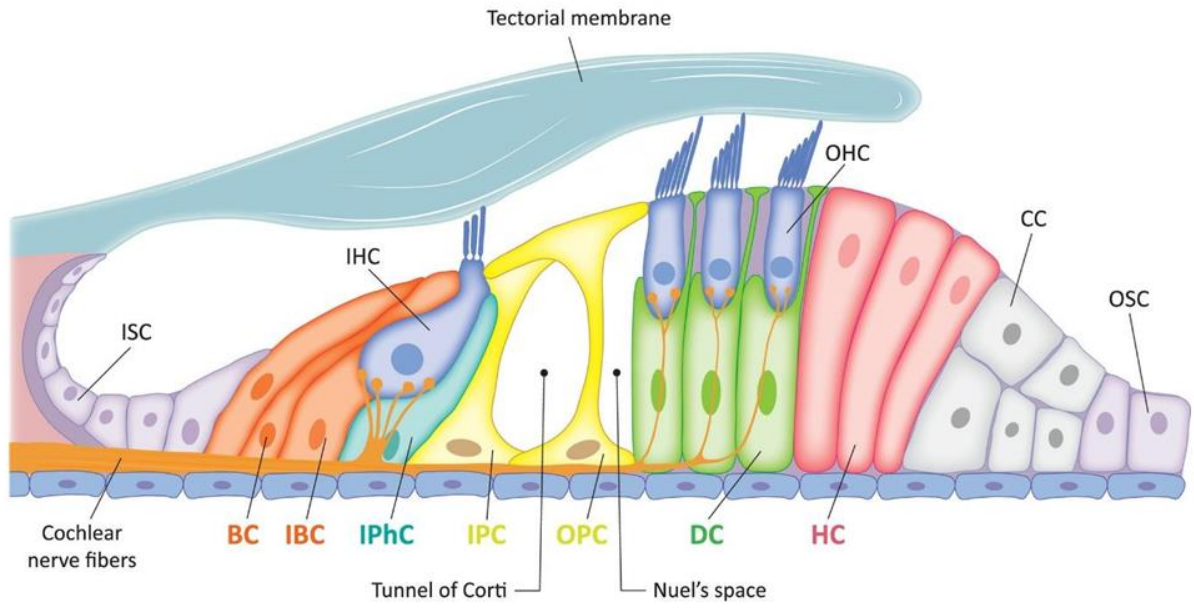

Figure 5: Supporting cells in the organ of Corti.

Providing structural as well as trophic support to the neighbouring HCs, a variety of supporting cells span the entire depth of the epithelium, forming a tight barrier to prevent fluid leakage. ISC/OSC: inner/outer sulcus cells; IBC: inner border cells; IPhC: inner phalangeal cells; IPC/OPC: inner/outer pillar cells; DC: Deiter's cells; HC: Hensen's cells; CC: Claudius cells. From Jang et al.

C. Innervation of the organ of Corti

The HCs are innervated by bipolar spiral ganglion neurons. Two types of these afferent neurons exist, type I neurons (90-95%) make unitary synaptic contacts with IHCs and convey sound signal, while type II neurons (5-10%) connect multiple OHCs “en passant” and are rather thought to play a role in nociception (Appler and Goodrich 2011). In addition to the ascending nerves projecting to the brain, the HCs also receive descending inputs from efferent neurons to control type I SGN and IHC excitability or OHC motility. By releasing neurotransmitters such as acetylcholine, or dopamine (Fuchs and Lauer 2019), the cochlear efferent system regulates hearing sensitivity, enhances the discrimination of speech in noisy background and could protect hearing from acoustic trauma.

1.3. Stria Vascularis and Spiral ligament

The stria Vascularis (SV), which laterally borders the scala media (Figure 2), is a multilayered secretory epithelium which plays a key role in maintaining the K^+ concentration high in the endolymph (Dufek et al. 2020). It comprises the basal, intermediate, and marginal cells and is highly vascularized. Potassium is reabsorbed by fibrocytes present in the spiral ligament, the connective tissue surrounding the SV, before being sent to the basal cells of the stria vascularis (Suzuki et al. 2016). There, the K^+ ions will go through a multitude of channels leading to its secretion in the endolymph. This process is extremely important as, without potassium in the endolymph, the HCs cannot get excited leading to deafness.

1.4. Extracellular Matrix

The inner ear comprises not only a wide variety of cells but also a rich extracellular matrix (ECM), which is vital to the hearing organ structure and function. Typically, the ECM is composed of glycosaminoglycans, such as hyaluronic acid (HA) responsible for compression resistance, and contains laminins and fibronectin, important for interactions within ECM molecules (Abatangelo et al. 2020). Proteoglycans also exert important water retention properties while collagens confer tensile strength and elasticity to the tissue (Lee-Thedieck, Schertl, and Klein 2022). In parallel to these mechanical roles, the ECM has also been shown to play a primordial role in signalling. Indeed, molecules such as proteoglycans are able to sequester important cell growth factors such as TGF-β while other ECM components such as HA, which will be discussed extensively in the following paragraphs, can directly interact with cell surface receptors to induce specific cellular responses (Schaefer and Schaefer 2010). The cochlear ECM is no exception, as it provides structural and biochemical cues to ensure otic development, homeostasis and function (Pressé, Malgrange, and Delacroix 2024) (Figure 6). Despite common components, such as collagens II

and IV, being found across tissular compartments, their organisation heavily varies with certain ECM types being highly specialised, including the resonant membranes, which will be discussed hereafter (Ishiyama et al. 2009).

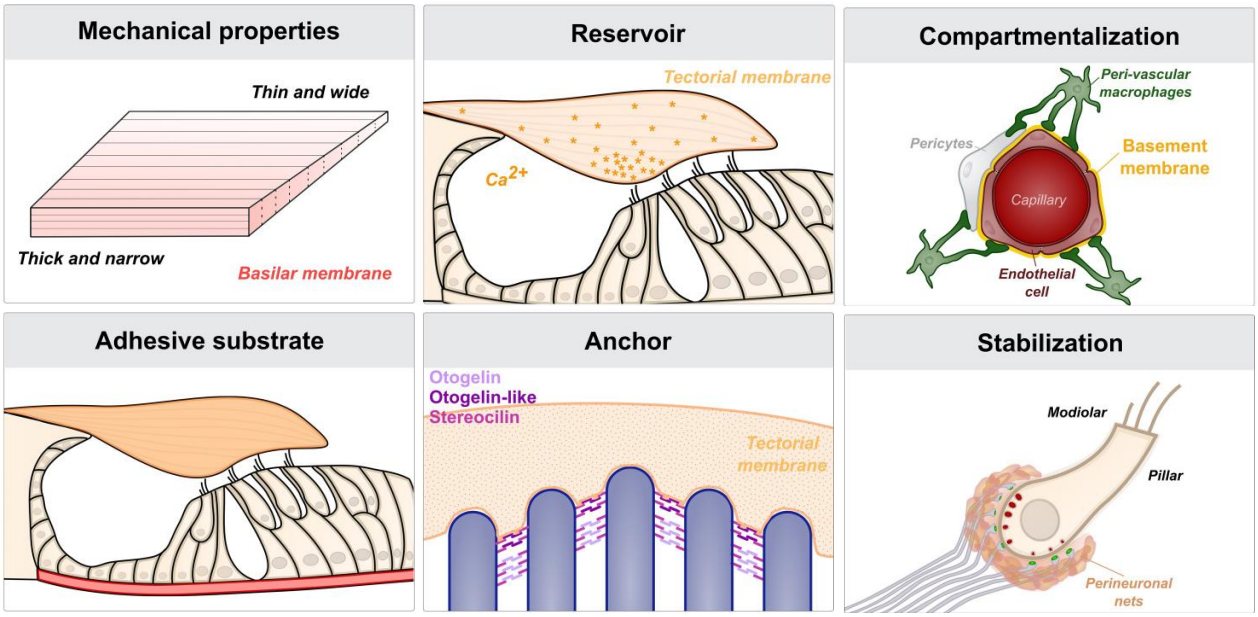

Figure 6: Cochlear ECM fulfils instrumental roles in the inner ear.

The basilar membrane is a highly specialized ECM whose topology and composition govern its vibrational properties, essential for cochlear tonotopy. It also plays an adhesive role for epithelial cells and a barrier function for cochlear fluids. Exclusively made of ECM, the tectorial membrane anchors OHC stereocilia to force their deflexion, additionally it acts as a Calcium reservoir for the sensory HCs. Other structures are physically insulated or stabilized by ECM, such as cochlear capillaries and synapses, respectively. From Pressé, Malgrange and Delacroix 2024.

A. Basilar membrane ECM

The BM is the ECM layer underlying the HCs, encompassing important roles for hearing, notably hair cell stimulation and sound-frequency decoding. It is mainly composed of structural proteins such as type IV collagen, and adhesive glycoproteins laminin β-2 and nidogen-1 (Liu et al. 2015). The organisation of this layer is crucial as mutations in proteins responsible for collagen fibril arrangement, such as Emillin-2, have been shown to induce hearing loss (Russell et al. 2020). The thickness and width of the BM vary along the longitudinal axis of the cochlea, with its width increasing and its thickness decreasing from the basal region to the apex. These topological variations, play a crucial role in determining the vibrational properties of the BM and establishing cochlear tonotopy as mentioned previously. This explains why the apical region preferentially

responds to lower frequencies while the basal region responds to higher frequencies. Moreover, it acts as a barrier, located between the scala media and scala tympani, ensuring fluid and ion regulation between the endolymph and perilymph (Pressé, Malgrange, and Delacroix 2024).

B. Tectorial membrane ECM

The TM is an acellular gel-like structure mainly composed of water (97%) which towers over the hair cells and is medially fixed on the Spiral Limbus. The TM comprises different types of collagens (type II, IV & XI mainly) as well as non-collagenous proteins such as TECTA and otogelin (Goodyear and Richardson 2018). These proteins are crucial for TM structure and fixation on the OHCs' hair bundles, ensuring proper stereocilia displacement upon sound stimulation. In TECTA null mice, the TM is no longer attached to the surface of OHCs resulting in mild to severe hearing loss (Jeng et al. 2021). Interestingly, the stiffness of the TM increases from the apex to the base, playing an important role in cochlear tonotopy. Other roles include modulating OHC cochlear amplification (Gavara and Chadwick 2009). Recently, it has also been shown to contain calcium, which allows the TM to influence excitability of the hair cells through modulation of calcium levels in the sub-tectorial fluid (Strimbu et al. 2019).

C. Cochlear capillaries and synapses

The spiral ligament and the stria vascularis contribute to cochlear blood supply as they are highly vascularized. These cochlear capillaries are surrounded by an ECM layer similar to other endothelial basement membranes (Tsuprun and Santi 2001). This ECM barrier contributes to the blood-labyrinth-barrier, which limits the diffusion of compounds from blood to cochlear tissue.

Recently a specific ECM network, named perineural nets, was identified around cochlear synapses (Sonntag et al. 2018). This basket-like structure is made of an HA cytoskeleton coupled to HA-linkers, brevican and Tenascin-R. The precise role of these ECM nets remains to be determined, however they are believed to stabilize synapses by ensuring the spatial coupling of pre- and post-synaptic machineries and thus neurotransmission.

2. ECM and Deafness

Deafness is defined as a shift in hearing threshold above 20 dB, ranging from mild to profound deafness (Anastasiadou and Al Khalili 2024). The impairment can range from having a hard time overhearing conversations to being unable to communicate properly with others, leading to social isolation. According to the WHO, currently, 1.3 billion people, nearly 20% of the world population, suffer from deafness, with 430 million of these experiencing complete deafness. Deafness can be of genetic origin, with both syndromic and non-syndromic forms, or of acquired origin, notably

through ototoxic drugs, noise exposure and aging. Most of these hearing impairments are sensorineural types, meaning they originate from defects in the cochlea.

2.1. ECM genes and hereditary deafness

Over 140 deafness-causing genes have been identified in humans, many of those being ECM-related genes (Figure 7). Syndromic hearing loss, which affects not only the inner ear but other organs as well, have been identified in patients encompassing mutations in genes such as collagens (namely type II and type IV collagen) for Alport and Stickler syndrome or cadherin 23 for Usher syndrome (Shin and Gillespie 2009; Mochizuki et al. 1994). Conversely, non-syndromic hearing loss, which affects the inner ear exclusively, includes mutations targeting cochlea-specific ECM components. A wide variety of genes have been identified in patients, notably Otogelin and TECTA (Schraders et al. 2012; Naz et al. 2003). Stereocilin mutations have also been denoted in patients suffering from hearing loss as it is an essential TM-OHC attachment protein (Verpy et al. 2001).

2.2. ECM and acquired forms of HL

A. Ageing

During the ageing process, many physiological changes occur in the human body. In the inner ear, these changes can affect a range of compartments including the ECM, whose degradation or accumulation overtime can ultimately lead to age related hearing loss (ARHL). Studies in humans have shown an increase in the ECM thickness around the capillaries located in the SV, which is suspected to be due to laminin deposition (Dufek et al. 2020). Other studies have shown a fibrocyte pathology leading to type II collagen loss in the lateral walls of aged mice cochleae, suggesting that ECM gene mutations potentiate ARHL (Buckiova, Popelar, and Syka 2006). Furthermore, RNAseq data highlighted ECM organization as one of the main pathways affected when comparing 6-week-old to 1-year-old mice (T. Zhao et al. 2020). Recently, a genome-wide association study also associated mutations in MMP2 with ARHL, highlighting the importance of ECM remodelling in ageing cochlea (Liu et al. 2021).

B. Noise exposure

Noise induced hearing loss accounts for the largest proportion of acquired forms of hearing loss in individuals under 40 years old. This specific type of hearing loss is due to high acoustic stimulation over long periods of time resulting in damage to important cellular and non-cellular cochlear structures. The most obvious target of this damage are the sensory hair cells, which can be targeted at multiple levels such as cell membrane or hair bundle integrity (Hu 2012). Other

structures, although less extensively studied, can also be affected such as the supporting cells and stria vascularis, crucial for ion homeostasis of the endolymph and perilymph. Finally, the damage can also target important ECM structures, such as the TM. Changes to the TM can range from decreased thickness to breaks or interruptions, which, of course, lead to improper hair cell activation following sound stimulation (Jeng et al. 2021). Studies show dysregulation of some ECM remodelers, namely the gelatinases MMP2 and MMP9, as well as ECM breakdown following noise overexposure (Wu et al. 2017; Jongkamonwiwat et al. 2020).

Overall, we can easily understand how important the ECM is to the hearing function as many of its components constitute potential targets for noise exposure or age-related damages, ultimately leading to cochlea dysfunction. In humans, an array of ECM-related genes is known to be causative of hearing loss, but many others remain to be investigated as genetic variation have only been correlated with disease in patients (Nishio et al. 2015). In this line, our research unit is currently investigating the importance of CEMIP and the gelatinases MMP2 and MMP9, to determine whether they are deafness-causing genes.

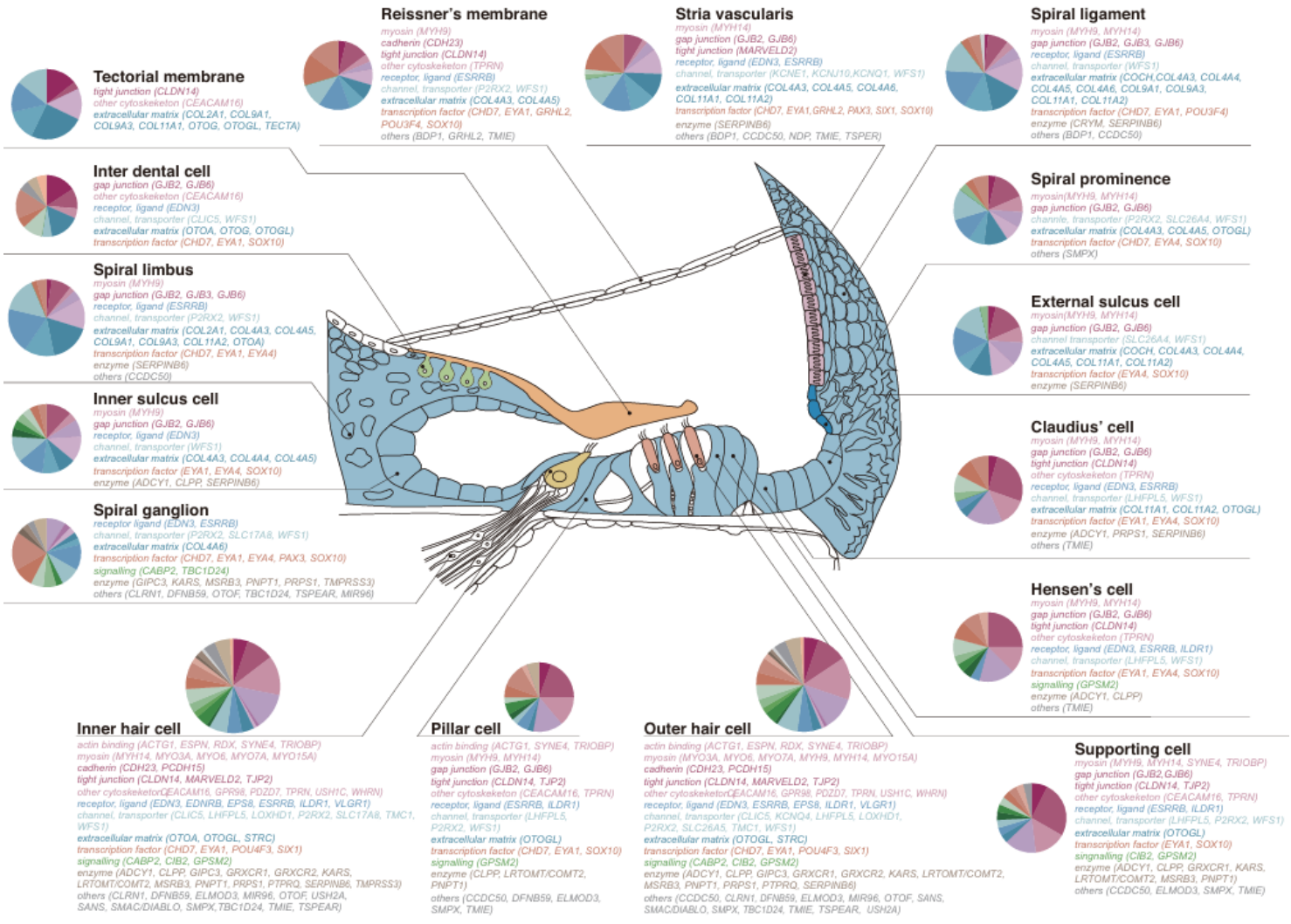

Figure 7: Genes involved in hereditary hearing loss and localisation of their protein product in cochlea.

Pie charts represent the cellular processes in which the mutated genes take part for each tissular compartment. Adapted from Nishio et al. 2015.

2.3. Hyaluronic acid and Cemip.

A. HA structure & function.

Hyaluronic acid (HA), also referred to as Hyaluronan, is a long linear chained glycosaminoglycan (GAG) composed of repeating disaccharides of D-glucoronate and N-acetyl-D-glucosamine, attaining a molecular weight of up to 2 x 10^7 Da (Neuman et al. 2015). HA is negatively charged and highly hydrophilic, allowing it to exert great water retention properties, conferring compression resistance to the ECM as well as modulating its visco-elastic properties (Kobayashi, Chanmee, and Itano 2020). HA also plays a role in maintaining the global architecture of the ECM and heavily contributes to allowing the ECM to return to its normal state, with no deformation, after stress.

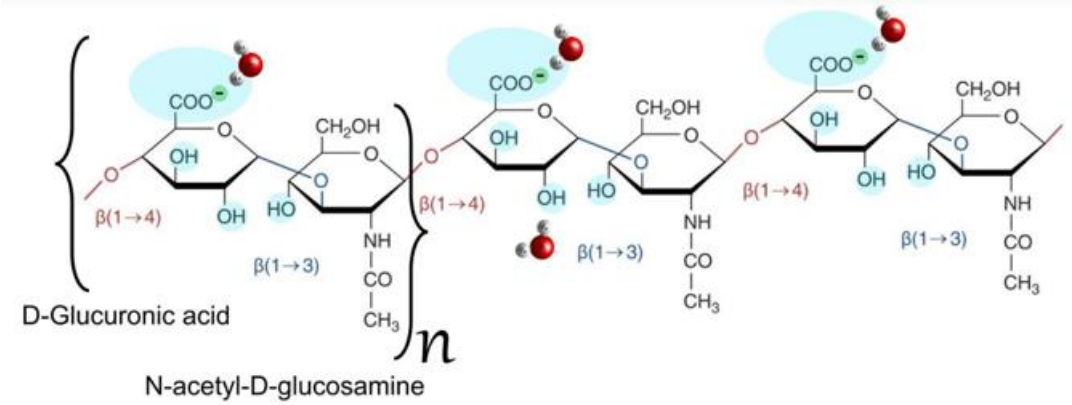

Figure 8: HA structure.

HA polymers are composed of repetitions of D-Glucuronic acid and N-acetyl-D-glucosamine disaccharides joined by β (1→4) bonds. Adapted from Jiang et al.

Naturally, HA can be found in many tissues, especially in embryonic tissue, cartilage, skin and adult soft connective tissue (H. Kim et al. 2019). While HA is mainly extracellular, intracellular forms have been reported although its functions haven't been fully elucidated yet. Unlike other GAGs, HA does not covalently bind to any protein to form proteoglycans but can rather be found at variable molecular weights, greatly influencing its function (Pressé, Malgrange, and Delacroix 2024). Fragments of sizes inferior to 250 kDa are referred to as low molecular weight (LMW) HA, fragments of sizes comprised between 250 and 1000 kDa as medium molecular weight (MMW)

HA, and fragments of sizes superior to 1000 kDa as high molecular weight (HMW) HA. For instance, HMW HA can be found in the synovial fluid of many articulations, where it is essential for lubrication (Hashizume and Mihara 2010). In addition to its crucial mechanical action, HA also exerts signalling functions that, once again, are influenced by its size. HA can interact with many different receptors, the main ones being CD44 and RHAMM, triggering pathways involved in cell proliferation, differentiation, and cell motility (Machado, Morais, and Medeiros 2022). Large HA polymer has also been shown to have anti-inflammatory properties while the LMW HA molecules are shown to have pro-inflammatory, angiogenic properties, pointing to opposing roles according to the size of the fragments generated through synthesis or degradation processes (Abatangelo et al. 2020).

B. HA metabolism.

Unlike other GAGs, HA is not synthetised inside the Golgi apparatus but rather at the surface of the cell before being released into the ECM (Rilla et al. 2005). The three main enzymes responsible for the synthesis of HA are HAS1, HAS2 and HAS3, expressed on the inner side of the cell membrane, allowing for both synthesis and translocation of HA to the ECM (Bart et al. 2015). These enzymes produce HA fragments of variable sizes with HAS1 and HAS2 producing large-sized fragments and HAS3 synthesizing smaller fragments (Itano et al. 1999). These enzymes are not the only ones that explain the different sizes of extracellular HA as a wide variety of catabolic enzymes also play a determining role. The enzymes degrading HA notably include HYAL1, HYAL2, HYAL3, HYAL4 as well as TMEM2 and CEMIP (Spataro et al. 2023). As the main HA degrading enzymes, HYAL1 and HYAL2 seem to be expressed in all somatic tissues while HYAL3 is mainly expressed in the testis and bone marrow. They catalyse the hydrolysis of the β1-4 glucuronic bond between two successive disaccharides of HA. CEMIP, a 150 kDa enzyme sharing no structural homology with the HYALs, is also involved in HA degradation. Evidence suggests that CEMIP acts intracellularly, through a clathrin-dependent pathway although it is also able to degrade HA in the ECM (Yoshida et al. 2013). Thanks to a signal sequence, this enzyme can degrade HA fragments extracellularly when it is secreted. Finally, HA polymers can also be degraded non-specifically by oxidative damage relating to ROS production.

C. HA, Cemip and hearing.

HA is speculated to play a crucial role in cochlear development and maintenance as many mutations of genes involved in its metabolism, namely HAS1, HYAL2 and especially CEMIP, have been found in patients suffering from hearing loss (Abe, Usami, and Nakamura 2003; Umugire et al. 2022). Studies conducted on HYAL2-/- mice confirmed HYAL2 importance in controlling otic

HA levels and function, as they have shown a significant hearing loss in 8- to 12-week-old mice (Muggenthaler et al. 2017). However, it remains unclear whether this hearing loss is of conductive or sensorineural origin. Originally, CEMIP expression was thought to be inner-ear specific with studies highlighting the presence of CEMIP in the spiral ligament and limbus in neonatal mice. Previous results from our lab confirmed the presence of Cemip in these two regions but also highlighted its expression in the sensory epithelium around HCs (Figure 9, left panel). Cemip hyaluronidase importantly contributes to HA degradation in this cochlear region since, in Cemip KO mice, we found ectopic accumulation of the polymer in the BM underlying the sensory HCs (Figure 9, right panels). As the deafness-associated mutations in humans are thought to disrupt the catalytic activity of Cemip hyaluronidase, we speculated that HA accumulation in the developing cochlea could alter the viscoelastic features of the BM, thereby impairing HC activation (Yoshida et al. 2014).

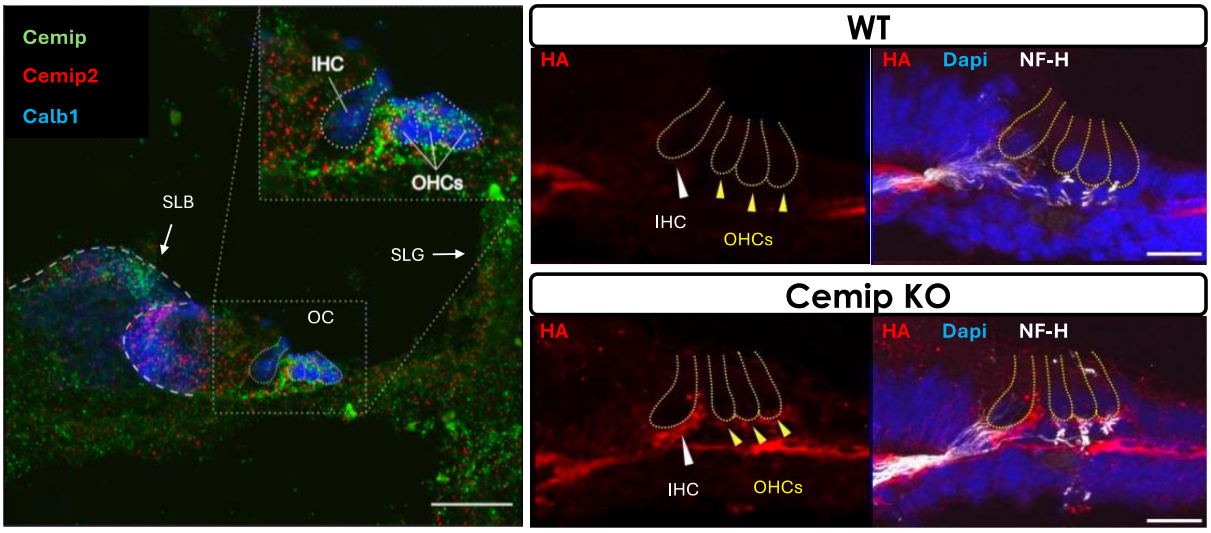

Figure 9. *Left panel:* RNAscope performed on neonatal mouse cochlea to detect Cemip (green) and Cemip2/TMEM2 (red) transcripts, combined with a Calb1 immunostaining to label the sensory HCs. The inset presents a magnification of the organ of Corti (OC). Scale bar= 50µm. *Right panels:* HA staining of WT and Cemip KO cochleae, combined with Dapi and Neurofilament-H antibody to label cell nuclei and SGN fibres, respectively. Scale bar = 20µm. SLB: spiral limbus, SLG: spiral ligament, IHC: inner hair cells, OHC: outer hair cells.

The role of Cemip was thus further explored at the functional level. Auditory brainstem recordings, or ABRs, have also been conducted by our team on 6-week-old mice to assess the hearing function in the absence of Cemip (Figure 10).

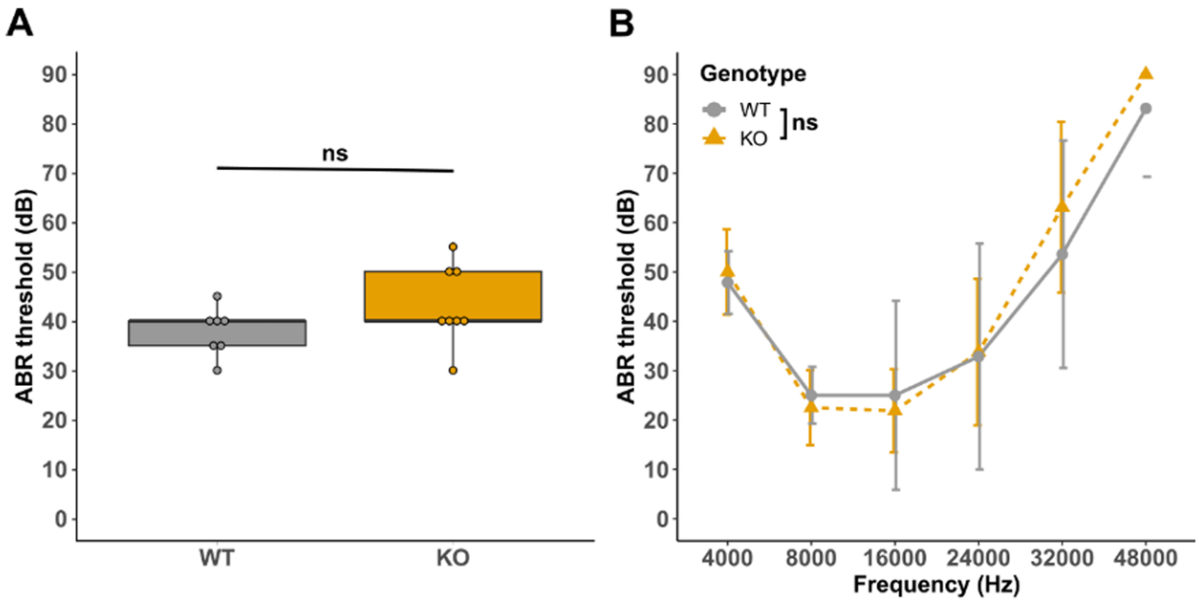

Figure 10: Hearing assessment of WT and Cemip KO mice at 6 weeks of age.

A. Auditory thresholds of WT and KO mice following a stimulation with a broadband sound (click). Mann-Whitney-Wilcoxon test. B. Auditory thresholds of WT and KO mice following a stimulation with pure tone sounds (4, 8, 16, 24, 32 kHz). Mean ± SEM. Two-way ANOVA. n=7 WT, n=8 KO.

Although Cemip is considered as a deafness-causing gene in humans, no differences in hearing thresholds could be evidenced in Cemip-deficient mice compared to control littermates, neither for click sound stimulation (mix of a broad range of frequencies), nor for pure tone sound stimulation. Young animals are thus able to hear correctly even in the absence of Cemip, nevertheless, this hyaluronidase could be potentially involved in cochlear maintenance during adulthood and ageing, as its expression persists in WT mice up to 1 year of age. Hence, to complete our study of Cemip hyaluronidase function in mice, its long-term importance on the cochlear function of aged animals still demands further investigation.

2.4. Metalloproteinases

A. MMPs function

Matrix metalloproteinases (MMPs) are enzymes able to degrade all kinds of ECM proteins and are therefore active ECM remodelers, important for tissue homeostasis but also playing a role in response to stress or damage. In addition, MMP endopeptidases can process other bioactive molecules, such as ligands, receptors, growth factors or cytokines, thereby regulating numerous signalling pathways. They intervene in many physiological processes such as cell proliferation, differentiation, migration and host defence (Bonnans, Chou, and Werb 2014). MMPs have been

linked to a variety of pathological processes, notably cancer, where they play crucial roles, both preventing and enabling cancer progression. These conflicting roles of MMPs are not uncommon as, upon inflammation, MMPs are crucial for tissue repair at first but can exert negative effects if the inflammation persists, expanding the original damage to the tissue (Frantz, Stewart, and Weaver 2010). MMPs can either be soluble or membrane-bound and they are initially synthetized as pro-enzymes that require proteolytic cleavage to ensure that the MMPs are activated. Typically, MMP activity is low but, following inflammation or other cellular stresses, their expression and/or activity rises. There are about 23 MMPs spread across 7 families, which are grouped according to sequence homology (Lu et al. 2011). Amongst them, MMP2 and MMP9 form a singular family, the gelatinases.

B. MMP2 and MMP9 structure

As mentioned previously, MMP2 and MMP9 share common protein domains (figure 11). First, the signal sequence, an essential part of these proteins, allows for them to be directed to the right cellular compartment which is generally secretion. The pro-domain prevents the MMPs from being active as it physically blocks their catalytic site (Bonnans, Chou, and Werb 2014). Therefore, MMPs themselves require cleavage to be active. In the case of MMP2 and MMP9, this activation can be done by other MMPs, such as the membrane-bound MMP14, also called MT-MMP1, by serine proteases and can even be mediated through an atypical pathway involving Tissue Inhibitor of Metalloproteinases (in this case, TIMP2), although these enzymes generally act as inhibitors of MMPs as we will discuss shortly hereafter (Shiryaev et al. 2013). Respectively, the pro and active forms of MMP2 have a molecular weight of 72 and 66 KDa while MMP9 forms attain 92 and 86 KDa. Their catalytic region is crucial for them to cleave other proteins and contains a Zinc ion, necessary for catalytic activity (Bassiouni, Ali, and Schulz 2021). Finally, a linker region joins these regions to the Hemopexin (HPX) domain, which participates in their interaction with other ECM proteins although its function is not completely elucidated yet. The main substrates of MMP2 and MMP9 include collagens (type II, IV, and X), fibronectin, laminins and elastin. These substrates are of course key proteins of the ECM, especially in the inner ear where mutations in some of these proteins (such as collagen 4) have been associated with hearing loss.

Figure 11: Schematic representation of MMP2 and MMP9 main substrates and their domains, including the signal sequence for secretion (S), the propeptide which has to be cleaved for activity (propeptide), the catalytic region and hemopexin (HPX). Adapted from Bonnans 2014.

C. MMPs and hearing

As MMPs are essential ECM remodelling enzymes, it is plausible that they play a role in audition, notably by altering the viscoelastic properties of the TM and BM inside the cochlea, by regulating cell support and signalling, or disrupting barrier functions. Since their activity is enhanced following inflammation or injury, which both occur upon ageing and noise overexposure, MMPs could also be important players in the ECM breakdown that accompanies noise-induced and age-related hearing loss. Amongst the metalloproteinases, MMP2 and MMP9 stand out as particularly interesting candidates, as they are expressed in multiple cochlear compartments and degrade collagen types that are predominant in the inner ear and crucial to the auditory organ (Wu et al. 2017). Their expression and/or activity is also rapidly and strongly modulated following noise trauma. In addition, MMP9 cochlear accumulation has been associated with hearing loss in mouse models of Alport syndrome (Gratton et al. 2005) and hyperhomocysteinemia (Kundu et al. 2009). Finally, in humans, MMP2 has been associated to age-related hearing loss in a genome wide association study (GWAS) done in 2021 (Liu et al. 2021). In our laboratory, preliminary experiments have been performed to investigate the spatio-temporal expression pattern of gelatinases in the cochlea (Figure 11).

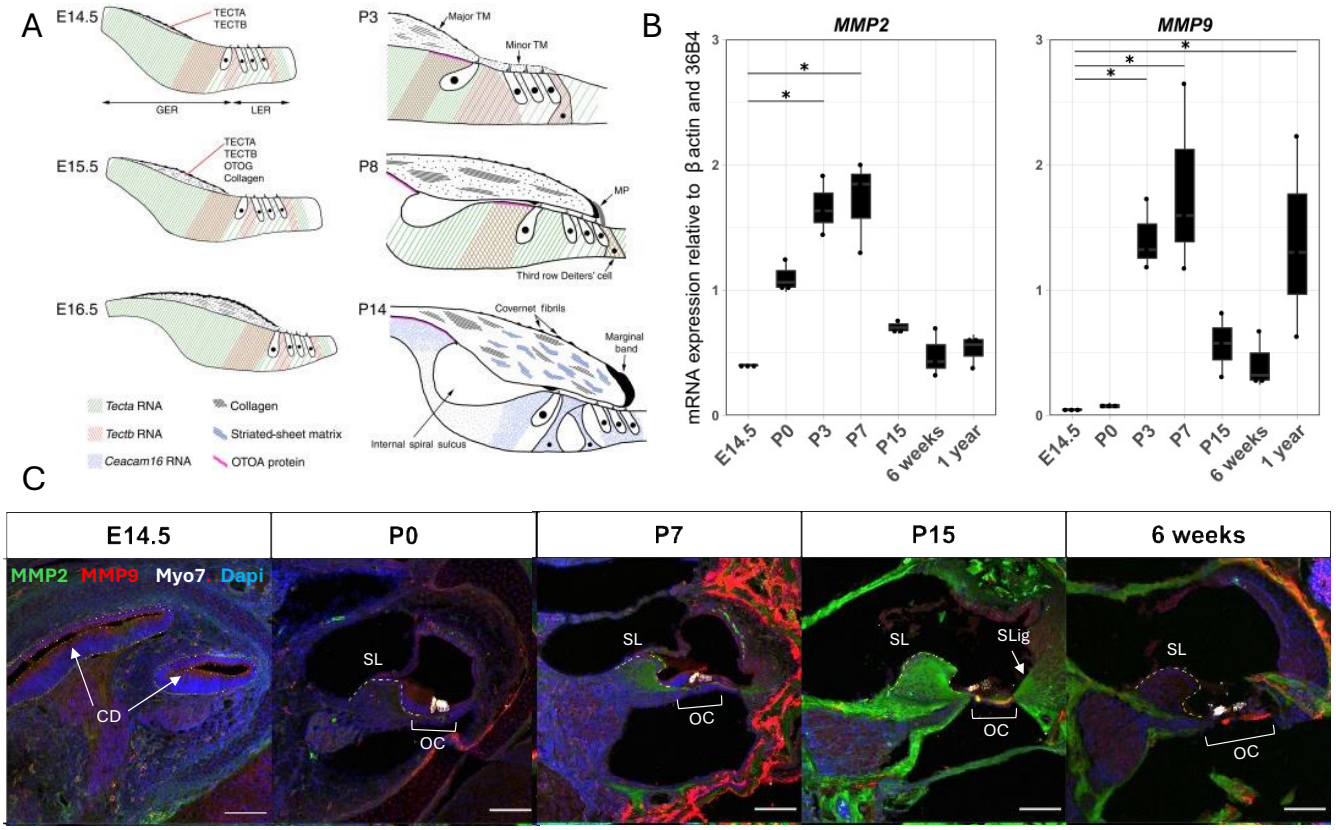

Figure 12: MMP2 and MMP9 expression profile in the developing cochlea.

A. Representation of cochlear development from E14.5 to hearing onset (P14). TM builds up above epithelial cells during embryonic stages, but the two first postnatal weeks are crucial for its maturation. During this period, cell shape changes and extracellular spaces are created in the organ of Corti in order to mature into a functional organ of hearing.

B. RT-qPCR indicating MMP2 and MMP9 transcript levels in the entire cochlea at different stages.

C. Immunostainings showing protein levels and localisation of MMP2 (green) and MMP9 (red) in the cochlea from E14.5 to 6 weeks. Myo7 antibody was used to visualise HCs and Dapi to stain cell nuclei. CD: cochlear duct, SL: spiral limbus, OC: organ of Corti, SLig: spiral ligament. Scale bars= 50 µm.

The transcript level of MMP2 in the entire cochlea increases from embryonic day E14.5 up to P7 and then drastically decline to basal levels from P15 onwards (Figure 12.B). MMP9 mRNA levels follow a similar trend, peaking at P7, however expression was also found to be increased at old ages. These expression profiles suggest they could play instrumental roles during the postnatal period of maturation before hearing onset, when TM detaches from the epithelium and cell reorganization in the organ of Corti leads to the creation of extracellular spaces. Immunostainings of the developing cochlea confirms that MMP2 and MMP9 expression is weak from embryonic stage E14.5 up to birth, with MMP9 being transiently enriched in the otic capsule at P7. At this stage, MMP2 is present in many structures with stronger staining in the spiral limbus and spiral ligament. MMP2 further accumulates in these regions to reach its maximal intensity at P15, which corresponds to the hearing onset in mouse. At this mature stage, both MMP2 and MMP9 proteins are present in the organ of Corti, below the sensory HCs. Later on, in young adults, MMP9 is still highly present in the bony structure surrounding the cochlea, while MMP2 remains strongly expressed in structures bordering the spiral ganglions as well as in the vestibular and tympanic ramps. Whether both MMPs are involved in the development of the cochlea and the hearing function will be investigated soon in our lab, as knockout mouse models are available. Nevertheless, strong evidence suggests a link between MMPs, hearing loss and ECM remodelling during adulthood, and given the importance of noise induced hearing loss, it appears essential for us to investigate the effects of noise exposure on these enzymes.

Aims of the work

The ECM intervenes in cochlear function by ensuring cell adhesion, mechanical and trophic support, compartmentalization and cell signalling to induce cellular adaptation to changes or stress. Therefore, ECM regulators are primordial for cochlear development and maintenance to guarantee proper hearing function and tissue homeostasis. As many human studies highlight deafness-associated mutations in ECM genes, it has become increasingly necessary to investigate the importance of these proteins for cochlear homeostasis. I focused on Cemip hyaluronidase for the first half of my project and on MMP2 and MMP9 gelatinases for the second.

Mutations in Cemip gene, an HA degrading enzyme, have been identified in patients suffering from hearing loss. To understand the role of Cemip in audition, our laboratory previously investigated its expression profile during cochlear development and generated a knockout mouse model to assess the hearing function in the absence of this hyaluronidase. Results indicated that Cemip is enriched below the sensory HCs during the postnatal period of maturation. Furthermore, they could evidence local accumulation of HA in this cochlear region in Cemip-deficient mice. The first aim of my project was to characterize the HA synthases that could be responsible for HA deposition in the cochlea at hearing onset. We thus performed RNAscope assays to detect HAS1, HAS2 and HAS3 transcripts in P15 wild type mice. As previous functional tests demonstrated no hearing deficits of Cemip-deficient mice at 6 weeks of age, we planned to address the hearing function of mice at increasing ages. To do so, we recorded auditory brainstem responses (ABRs), which correspond to electrical signals emitted by the brain in response to sound stimulation, of WT and Cemip KO mice at 8 and 16 weeks of age.

Published studies highlighted MMP2 and MMP9 expression changes in noise exposed cochleae. Hence, we speculate these gelatinases could play a primordial role in ECM remodelling following noise trauma, and my project was dedicated to further investigate their implication. First, we characterized a noise-induced hearing loss mouse model by analysing, through ABRs, the hearing function of mice following sound exposure and checking, by immunostaining and RT-qPCR, if an inflammatory response was triggered. Finally, I analysed MMP2 and MMP9 expression changes at the transcription and protein levels, by RT-qPCR and immunostaining, respectively.

Material and Methods

1.1 Animals

CEMIP KO mice

Cemip flox mice were obtained from Cyagen by flanking exon 4 and exon 5 with LoxP sites, which upon CRE expression, may be removed from genomic DNA. To this end, mice were crossed with $PGK^{cre/+}$ mice, which allowed for this recombination event to happen in all cells as this promoter is ubiquitous. This deletion of exons 4 and 5 triggers a frameshift and the subsequent introduction of a stop codon, stopping the synthesis of the protein prematurely.

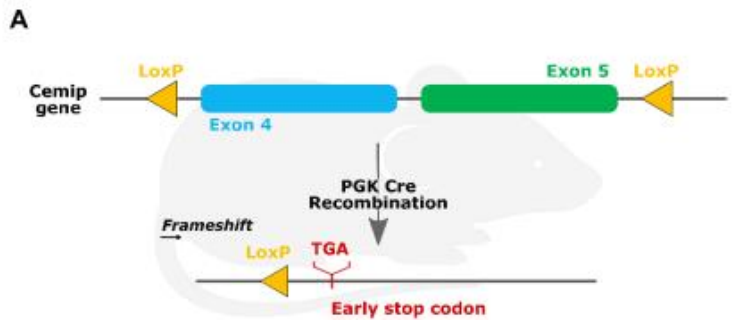

Figure 13: Cemip gene invalidation strategy.

$Cemip^{Lox/Lox}$ mice were crossed with a $PGK^{Cre/+}$ mouse line expressing Cre recombinase under the control of a ubiquitous promoter, allowing for the excision of exons 4 and 5 in Cemip gene. The recombination induces a frameshift and a premature stop codon, thereby generating a Cemip KO line.

Genotyping was performed as follows. A small piece of the tail of each mouse was sampled and digested using 3 µL of proteinase K (REF: V3021, 30 u/mg, PROMEGA) dissolved in 300 µL of TENS (TRIS 100mM, EDTA 5 mM, SDS 0.2% and NaCl 200mM). This reaction occurred at 55°C under agitation for 1-2h. Precipitation of genomic DNA is then realised using 300 µL of isopropanol 100% (REF: 20842.323, LOT 22A314035, VWR BDH CHEMICALS) and centrifuged at 13 000 rpm during 10 minutes at 4°C. After isopropanol removal, 600 µL of ethanol 70% (REF: 20821.310, LOT 22C174009, VWR BDH CHEMICALS) are added as a washing step and centrifuged with the same parameters. After removal of the supernatant, the DNA is resuspended with 300 µL milliQ water and stored at 4°C.

PCR was done using the SensoQuest Labcycler, following steps described in table 1. In microtubes, 1.5 µl of DNA were added to 0.2 µM of target gene primers (detailed in table 2), 5 µL

of reaction buffer 5X (Promega, #M7848), 200 µM of dNTP, 2 mM of $MgCL_2$ (Thermoscientific) and 5 units of GoTAQ polymerase (Promega - #M7848) in a final volume of 25 µL. PCR products were kept at 4°C before analysis using an agarose gel.

Table 1: PCR cycle for genotyping

Steps	**Duration**	**Temperature**
Pre-denaturation	3 minutes	95°C
Amplification *(35 cycles)*	20 seconds	95°C
	45 seconds	60°C
	30 seconds	72°C

Table 2: PCR primers for CEMIP

Name	Primers (5' → 3')
mCEMIP-F1_gen	CAG TTT CTA TTG GTG CTC TGA AGG GA
mCEMIP-R2_gen	TGT CAC CTG TAC CTC TGC ACC TC
mCEMIP-F3_gen	AGA GGA CTT CCC AGG GTG TG

1.2 Auditory brainstem response

Auditory brainstem response (ABR) was recorded on 6-week-old WT mice as well as 8- and 16-week-old Cemip KO and WT mice. They were placed on a heating pad inside an anechoic chamber, electrically and sound isolated. After being anesthetized using Ketamidor (Ecuphar 804131) (100 mg/ml) & Rompun 2% (Bayer BE-V041815), they were placed 10 cm away from the speaker (MF1 multi-field magnetic speaker TDT), which delivers sounds at 4kHz to 48kHz, ranging from 0 to 90 dBs. Three electrodes were placed underneath the skin of the mice. The recording electrode is placed at the vertex, the reference electrode on the ipsilateral side on the base of the ear and the ground electrode is placed on the contralateral side behind the ear. Recordings provide five electrical waves that are evoked by sound stimulation, they correspond to different neuronal relays from the periphery to the brainstem.

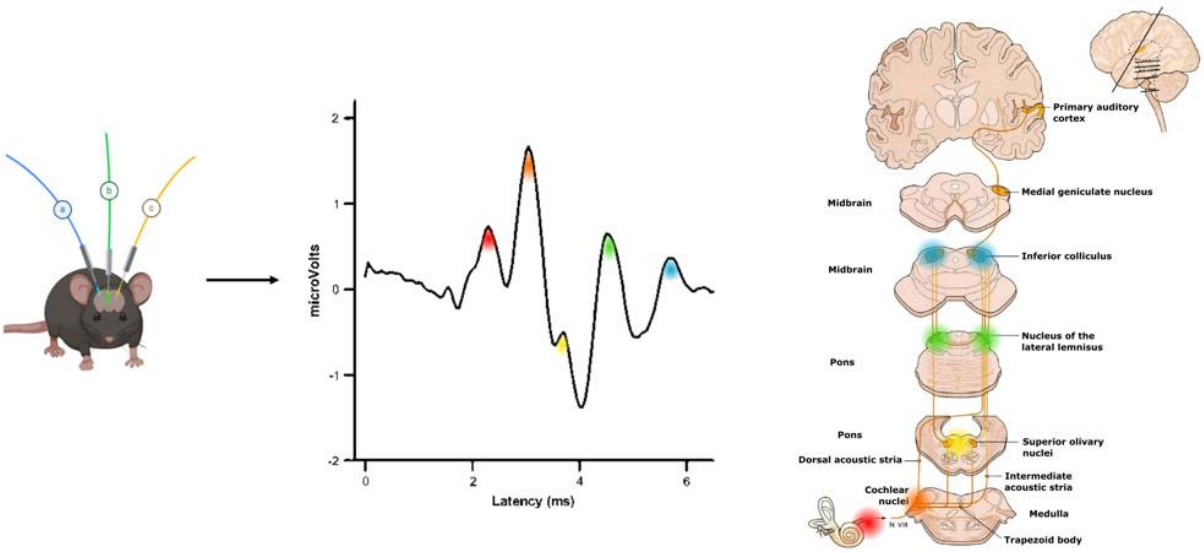

Figure 14: Auditory brainstem recording (ABR) illustrating the typical waveform recorded following sound stimulation. Each discernible peak corresponds to a neuronal relay in the auditory pathway, the first one corresponding to cochlear nerve (IHC-SGN activity).

Evoked potentials are measured in microvolts and assessed for each of the five peaks represented on the graph, namely the cochlear nerve, the inferior and superior olivary, the nucleus of the lateral lemniscus and finally the inferior colliculus.

Recordings and trace visualization are performed using the BioSig software (TdT Instrument). Hearing thresholds were determined as the minimal sound intensity at which we can see the stereotypical waves.

1.3 Trauma

Noise exposure experiments were conducted at Harvard University and cochlear samples were sent to our research facilities. Briefly, 6-week-old mice were exposed to noise trauma through a speaker for 2h, at 100dB and 8 to 16 Khz.

1.4 Tissue preparation and sectioning

From P15 to 6-week-old WT mice, the heads were dissected in PBS (biowest L0615 500) to remove the brain and extractthe cochlea. The bony cochleae were poked with forceps to create a hole through the apex and excess tissue was removed from the oval and round windows. They were then immediately placed in PFA 4% (ALDRICH 158127) and left overnight, at 4°C, under agitation. Cochleae were rinsed three times in PBS and incubated up to three days in EDTA 4%, at 4°C, under agitation. Afterwards, they were incubated in successive baths of 10, 20 and 30% sucrose (D(+)

Saccharose VWR chemicals 27478.365) overnight each time and finally embedded in OCT (Epredi 6502B) and stored at -80°C.

For P0 mice, their entire heads were fixed in PFA 4% for 24h. Afterwards, the heads were put in successive baths of sucrose 10% - 20% - 30% overnight until sinking. They were embedded in OCT and stored at -80°C until use.

Sectioning of the OCT embedded cochleae and heads was performed using the cryostat (Cryostar NX70, Epredia), cooled down at -20°C beforehand. For cochleae, sections of 16 µm were performed in the axis of the modiolus using a blade (Epredia 3053835) and antiroll brought to -20°C as well. Sections were placed on superfrost slides (Epredia J1800AMNZ) and left to dry one day under a fan before storage at -80°C. For the heads, sectioning was performed following the same procedure, in the axis perpendicular to the cochleae.

1.5 Immunofluorescence

Immunofluorescence was performed on frozen cochlear samples from P15 to 6W mice. They were washed using PBS containing 0.3% Triton (PBST), 3 times for 5 minutes and blocked using donkey serum (DS) 10% (Jackson Immuno Research 017-000-121) in PBST during 1h. We used different primary antibodies (see table below), which were incubated overnight at 4°C, in PBST containing 5% DS. After 3 washing steps of 5 minutes in PBS, sections were covered with the same buffer containing secondary antibodies and the nuclear stain (see table below) and left 1h in the dark at RT. Slices were mounted using a few drops of DAKO (Agilent Techbologies S3023) with a 20X58 mm slide (Knittel Glass coverslips). They were dried under a fan overnight and visualized the next day on the confocal microscope (Olympus FV1000).

Table 3: Primary and secondary antibodies for immunostainings.

Primary Antibody	CALB1	BioKé 13176S	Rabbit	1/500	Overnight at 4°C
	MMP 2	Santacruz (sc-13595)	Mouse	1/100	Overnight at 4°C
	MMP 9	Santacruz (sc-393859)	Goat	1/100	Overnight at 4°C
	bHABP	Amsbio (AMS.HKD BC41)	/	1/100	Overnight at 4°C
	Myosine VII a	ENZO Life sciences	Rabbit	1/500	Overnight at 4°C
	Neurofilament	EMD Millipore (MAB5448)	Rat	1/1000	Overnight at 4°C
	COL 4	ABCA4 (3F4) sc-65672	Rabbit	1/250	Overnight at 4°C
Secondary Antibody	Streptavidin	Invitrogen (S21381)	Donkey	1/250	1h at 4°C, covered
	Anti rat	Alexa Fluor	Donkey	1/1000	1h at 4°C, covered
	Anti rabbit	Alexa Fluor	Donkey	1/1000	1h at 4°C, covered
	Anti mouse	Alexa Fluor	Donkey	1/1000	1h at 4°C, covered
Nuclear stain	DAPI	Sigma (D9542)	/	1/1000	1h at 4°C, covered

1.6 RNAscope

RNAscope was performed on WT mice at P0 and P15. First, the tissue sections were air dried for 1h at RT, washed in PBS for 5 minutes before being backed overnight at 60°C. The next day, the slices were post fixed in PFA 4% at 4°C during 15 minutes before successive 5 minutes incubation steps in ethanol (50% - 70% - 100% - 100%) at RT and dried. For the following steps, the RNAscope® Fluorescent Multiplex Kit v2 (Advanced Cell Diagnostics) was used. Four to six drops of Hydrogen peroxide were added to the slides and incubated for 10 minutes. After removal by washing the slides three times in distilled water, the slides were incubated with 1X target retrieval reagent at 99°C for 5 min. Afterwards, they were rinsed in water for 15 seconds, washed in ethanol 100% for 3 min and dried at 60°C for 5 min before a hydrophobic barrier was drawn around the target tissue using the ImmEdge hydrophobic barrier pen. Five drops of Protease III were added to the section and left at 40°C during 30 min and washed 2 times in 200 ml of fresh water. Afterwards, 50 µl of the probe mix was added to the slides (see table A below for the probe mix) and incubated for 2h at 40°C before rinsing using 200 µL of Wash Buffer for 2 min. Successively, FL V2 AMPs 1, 2 and 3 were added for 30 min at 40°C on each slide with 2 wash steps of 2 minutes each using Wash Buffer after every AMP. A few drops of HRP C1 were then added to the slides for 15 minutes at 40°C before being washed 2 times and having the fluorochrome OPAL 488 added to them for 30 minutes at 40°C and washed again twice following the same instructions as previously. This step was then repeated for the HRP C2 and HRP C3, with the same washes, using the Opal 555 and 647 instead. Four to six drops of HRP blocker were then added to the slides for 15 minutes at 40°C and washed again. Immunofluorescence for CALB1 staining and DAPI nuclear staining were performed directly after this procedure (see Immunofluorescence protocol detailed previously).

Table 4: Probes used for RNAscope.

Target mRNA	Name	Reference	Channel
HAS1	RNAscope® Probe - Mm-Has1 - Mus musculus hyaluronan synthase 1 (Has1) mRNA	510511	C1
HAS2	RNAscope® Probe - Mm-Has2-C2 - Mus musculus hyaluronan synthase 2 (Has2) mRNA	465171-C2	C2
HAS3	RNAscope® Probe - Mm-Has3-C3 - Mus musculus hyaluronan synthase 3 (Has3) transcript variant 1 mRNA	483861-C3	C3

1.7 Confocal Imaging

Imaging of fluorescent immunostainings was done using the Olympus FV1000 Confocal, using the 10X and 40X objectives. Images using the 10X magnification were centred at the modiolus and images using the 40X magnification were centred on the organ of Corti. Image acquisition settings are identical between groups.

1.8 RNA extraction

Inner ears of 6-week-old mice were extracted and further dissected to isolate the cochlea from the otic capsule. Tissues were collected in 1.5 mL tubes, centrifuged to eliminate residual PBS, and 500 µl of Trizol (Invitrogen 15596018) were added before storing the samples at -80°C. For RNA extraction, samples were first scrambled using an electrical pestle (VWR, 47747-366) then 100 µl of chloroform (Roth Nr. CAS 67-66-3) were added to each tube. After mixing thoroughly, they were centrifuged at 12 000 g at 4°C for 15 minutes and the aqueous phase containing nucleic acids was collected and mixed with 500 µl of isopropanol (VWR chemicals 20842.323). After centrifuging at 12 000g for 10 minutes, the supernatant was removed and ethanol (VWR chemicals 20821.310) 75% was added to the pellet and centrifuged again at 7500 g at 4°C for 5 minutes. The pellet was resuspended in 40 µl of RNAse-free water and placed into the 55°C incubator for 10 minutes. Afterwards, DNase treatment was done by adding 5 µl of 10X buffer and 5 µl DNase I (Fisher EN0521) for 30 min at 37°C. Reaction was stopped using 5 µl d'EDTA 0.55 M for 10 min à 65°C. RNA concentrations were determined using Nanodrop before the tubes were stored at -80°C until RTqPCR.

1.9 RTqPCR

RT was performed on the samples using 300 ng of total RNA with the RevertAid First Strand cDNA Synthesis Kit (K1622, ThermoFisher). RNA was mixed with 1 µl of random primers and the solution was completed with water until reaching a total volume of 12 µl for 5 min at 65°C. Afterwards, 4 µl of reaction buffer 5X, 1 µl of RiboLock RNase inhibitor (20U/µl), 2 µl of dNTP mix (10 mM) and 1 µl RT (200 U/µl) were added to the tubes for 60 min at 42°C. The samples were then stored at -20°C for qPCR.

The qPCRs were performed in the 480 Lightcycler machine (Roche) using the GoTaq(R) qPCR Master Mix (Promega, A60002). The qPCR program as well as the primers used are recapitulated in the tables below. Briefly, 4 µl of 20-fold diluted cDNA samples were added to a 384 well plate with 5 µl of SYBR Green Super Mix and 1 µl of primer mix F/R 3 µM. All of the samples were done in triplicates for each gene tested.

To quantify the DNA concentration in each sample, we used the quantification method relative to a standard curve. In order to establish the standard curve, we added 10 µl of every sample diluted 20-fold to one unique tube and performed serial dilutions to obtain 6 standards. We determined the mean concentration value for each sample (technical triplicates) and normalized this value for every gene tested on that of the housekeeping gene 36B4. After this, as every timepoint is represented by 3 samples, except for the control represented by a unique sample (due to technical difficulties), the mean of the three biological replicates representing a unique timepoint was reported to control condition (pre-exposure).

Table 5: qPCR program.

Step	Duration	Temperature
Pre-incubation	10 minutes	95°C
Amplification *(45 cycles)*	10 seconds 45 seconds	95°C 60°C
Melting curve	15 seconds	95°C
	30 seconds +0.11°C/second (5 acquisitions / second)	60°C 97°C
Cooling	30 seconds	40°C

Table 6: qPCR primers.

Gene	Name	Target sequence	Target exons
36B4	m36B4qFex6	ATGGGTACAAGCGCGTCCTG	6 and 7
	m36B4qRex6-7	GCCTTGACCTTTTCAGTAAG	
B-Actin	mActb	CACTGTCGAGTCGCGTCC	1 and 2
	mActb	TCATCCATGGCGAACTGGTG	
MMP2	mMMP2qFex8	GGCTGGAACACTCTCAGGAC	8 and 9
	mMMP2qRex9	GTCAGTATCAGCATCGGGGG	
MMP9	mMMP9qFex1	CCGACTTTTGTGGTCTTCCC	1 and 2
	mMMP9qRex1-2	CGGTACAAGTATGCCTCTGC	
IL6	mIL6qFex2	GGATACCACTCCCAACAGACC	2 and 3
	mIL6qRex3	TTCTGCAAGTGCATCATCGT	

1.10 Statistical analysis

All the statistical analyses for the following experiments (ABRs and RTqPCRs) have been conducted using GraphPad (Prism 8.0.2). Proper statistical tests were done to verify normality of the samples to determine the use of parametric or non-parametric tests. Details on the individual statistical tests and multiple comparisons are provided below each figure/result obtained. * = $p < 0.05$, ** = $p < 0.01$, *** = $p < 0.001$ and **** = $p < 0.0001$.

Results

1.1. Investigating the role of cochlear HA and CEMIP on the hearing function

A. HAS1, 2 and 3 expression profile at hearing onset

Different enzymes are involved in HA metabolism, amongst them HAS1, 2 and 3 are enzymes capable of synthetizing new HA. In the lab, the expression pattern of these enzymes has been determined during embryonic and early postnatal stages of development, but limitations of the RNAscope protocol that we used at the time didn't allow us to investigate these enzymes at postnatal day 15 (P15), when the cochlea is fully mature, and hearing is operational. This was due to the decalcification steps that are necessary to soften the bony otic structure before cochlear sectioning, which prevented the probes from binding to their target RNAs. Now that we fine-tuned the protocol, we performed RNAscope on slices of P15 wild-type mice, to detect the transcripts of the three HAS genes. This assay was combined to CALB1 immunostaining to reveal the sensory HCs and the spiral limbus region as well as DAPI to label the cell nuclei, and we used P0 slides as a control. As we can see on figure 15, HAS1 is absent at both stages, which is in good accordance with previous RT-qPCR performed in the lab that failed to detect HAS1 transcript. In contrast, HAS2 and HAS 3 are expressed in P0 cochlea, as signal is detected in the sensory epithelium and spiral ganglion for both probes. Transcripts are specifically present in the region of Calb1-positive HCs and spiral limbus, and HAS3 is particularly enriched in SGNs. At P15, which corresponds to hearing onset, mRNA levels of HAS2 and HAS3 are significantly decreased compared to birth, however they are still found in cochlear epithelial cells and neurons, some of which are also labelled by Calb1 at this stage. These results suggest that HAS2 and HAS3 are the major enzymes responsible for HA accumulation during cochlear development, even during the first postnatal weeks during which functional maturation occurs.

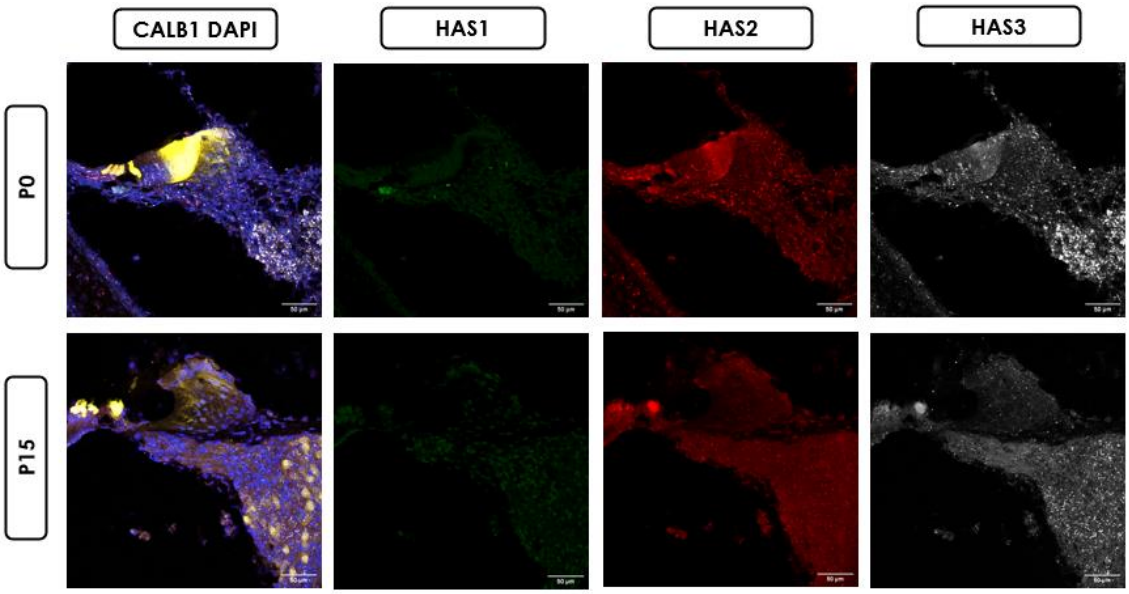

Figure 15: HAS1, 2 and 3 expression profile in the middle turn of WT cochlea at birth (P0) and upon functional maturity (P15). RNAscope probes for HAS1, 2 and 3 were combined to CALB1 immunostaining and DAPI staining of transversal sections of WT mice at P0 and P15. Images were taken with 40X magnification. HCs: hair cells; SL: spiral limbus; SGNs: spiral ganglion neurons, scale bars = 50 µm.

B. Evaluation of the auditory function of wild-type and CEMIP KO mice over time.

As detailed previously, CEMIP gene mutations have been identified in patients suffering from hearing loss (Abe, Usami, and Nakamura 2003). As we suspected it might play a key role in hearing function, our lab conducted investigations about the relevance of Cemip, but these were limited to 6-week-old mice and suggested that Cemip did not play a role in hearing function, as no difference were seen between wild type and KO mice. To assess whether Cemip could be required at later stages, for the maintenance of cochlear integrity during aging, we planned to conduct a longitudinal study of the hearing function of Cemip KO mice by performing ABRs at 8, 16, 24 and 32 weeks of age. Because of obvious time limitations, only the two first time points, which are 8 and 16 weeks, could be completed over the course of my Master Thesis project.

Hence, we performed ABRs, which allow us to record the electrical signals evoked in the brainstem of the mice in response to sound stimuli of increasing intensities (dB) and identified the hearing threshold as the minimal intensity at which the 5 typical peaks are discernible (Figure 15A). This response is measured for every sound intensity between 0 dB and 90 dB (with a 5 dB step size) and indicates whether the mice hear at each one of these sound intensities. The results presented in Figure 16B indicate the hearing thresholds of the different mice groups following a sound stimulus composed of mixed frequencies, usually referred to as click ABRs. They indicate no difference in hearing threshold between WT and KO mice at 8 weeks, as they are both able to respond to click sounds of 40 dBs. However, at 16 weeks, a significant hearing threshold elevation can be observed in KO animals when compared to WT littermates, suggesting that CEMIP invalidation negatively impacts the hearing function of 16-week-old mice. Noteworthy, the threshold of 16-week-old WT mice is abnormally low, being even lower than that of the 8-week-old mice in the wild type condition. This is surprising, as the hearing function should either remain stable or decline with time. .

We also performed the same test in Pure Tone conditions which, as opposed to broad clicks, are different sounds of precise frequencies (ranging from 4 to 48 kHz). The frequencies at which mice perceive sound best are usually situated between 8 to 24KHz, their hearing being worse for lower and higher frequencies. Thus, it is important to test frequencies inside and outside of their

optimum hearing range to ensure the test is as reliable as possible. At 8 weeks of age, we can see that KO mice have slightly elevated hearing thresholds for high frequency sounds (32 and 48 kHz), but the difference with that of WT mice is not statistically significant (Figure 16C, compare full red and black curves). As expected with increasing age, the hearing thresholds for 16-week-old mice are generally higher than those of the 8-week-old mice, for both groups (Figure 16C, compare solid and dotted lines). For high frequency sounds (24, 32 and 48 kHz), the threshold of 16-week-old Cemip KO mice is increased compared to that of WT mice at the same age, however the difference is not significant.

Collectively, our results indicate that Cemip depletion does not significantly affect the hearing threshold of mice up to 16 weeks of age. Future analyses, performed at older ages, will allow us to know if Cemip deficiency could accelerate or exacerbate age-related hearing loss.

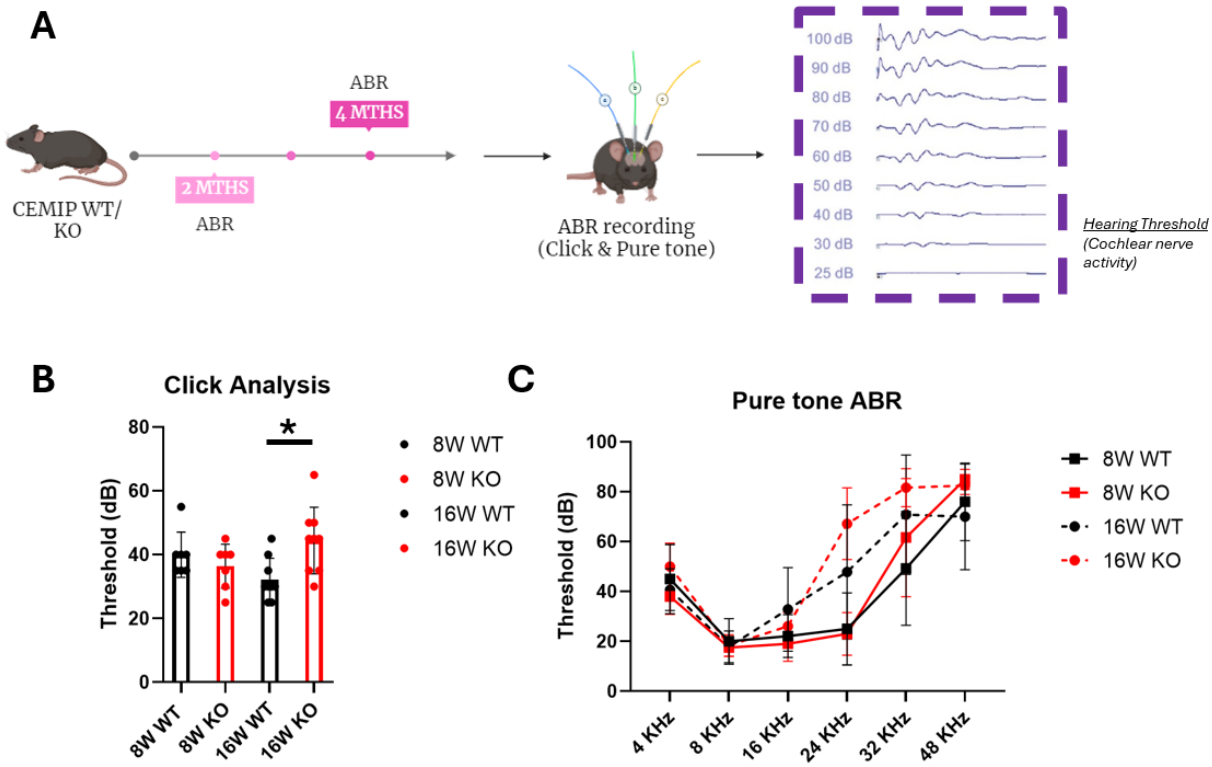

Figure 16. Effect of CEMIP invalidation on the hearing thresholds of 8-week and 16-week-old mice.

A. Experiment timeline.

B. Click ABR thresholds of WT and Cemip KO mice at 8 and 16 weeks of age. The individual data (n=7-9 per group) are presented in scatter plots with mean +/-SEM. Kruskal-Wallis was performed (pval=0.03) and post-hoc Dunn test was applied to compare all different groups (*pval<0.05).

C. Pure tone ABR thresholds of WT and CEMIP KO mice at 8 and 16 weeks of age. Mixed models ANOVA were performed (pval < 0,0001). Post-hoc Tuckey test reveals that 8-week KO thresholds are significantly different from those of 16W KO at 4 KHz (p val < 0.05) and at 24 KHz (p val < 0.0001).

1.2 Investigating the role of cochlear MMP2 and MMP9 on the hearing function

A. Effect of noise exposure on hearing thresholds of 6-week-old mice.

Noise exposure has been shown to induce damage to the cochlea, affecting hair cells or even the ECM, as shortly as 2 hours following the exposure. This damage can result in hearing loss, translated by an elevation of hearing threshold, which can be transient when the hearing threshold pre-exposure is recovered after a short period of time, or permanent when there is a "residual" hearing loss (Hu 2012). To investigate the hearing deficits of mice after being exposed to noise and verify our noise trauma protocol, we performed ABRs on 6-week-old wild type mice after having exposed them for 2 hours to 100 dB of sound from 8 to 16 kHz. These ABRs were recorded following clicks (mix of different sound intensities) as well as pure tones (individual sound frequencies) stimulation and the hearing thresholds were determined before noise trauma (D0) and 1-, 3- or 7-days post-trauma (D1, D3 or D7, see Figure 17A). The click ABR thresholds of C57Bl6 mice were of 35 dBs in average in pre-exposed animals (Figure 17B), consistent with previous results obtained in our laboratory and in the literature. After noise exposure, hearing thresholds tended to be transiently elevated, as they reached 50 dBs +/-15 dBs at D1 and D3, before being partially restored at D7 (40 dBs +/- 10 dBs). Although these click ABR tests suggest that our noise trauma protocol efficiently induced hearing deficits, the results were not significantly different between the various time points, probably because of high variability amongst the groups. Nevertheless, in Figure 17C, we can see that the pure tone ABR thresholds also increase at D1 and D3 as well as a partial restoration at D7, consistent with Clicks. Moreover, at certain frequencies (16, 24, 32 kHz), the transient elevation of the threshold was statistically significant at D1 and D3, thereby confirming that noise exposure affected the hearing function.

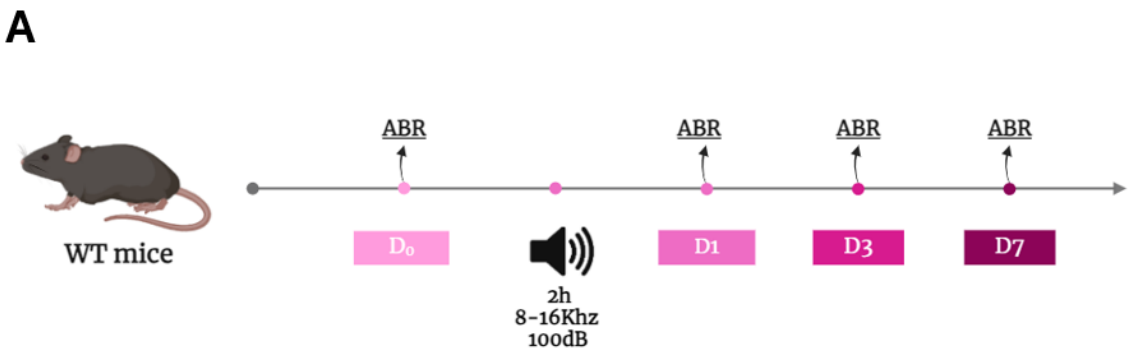

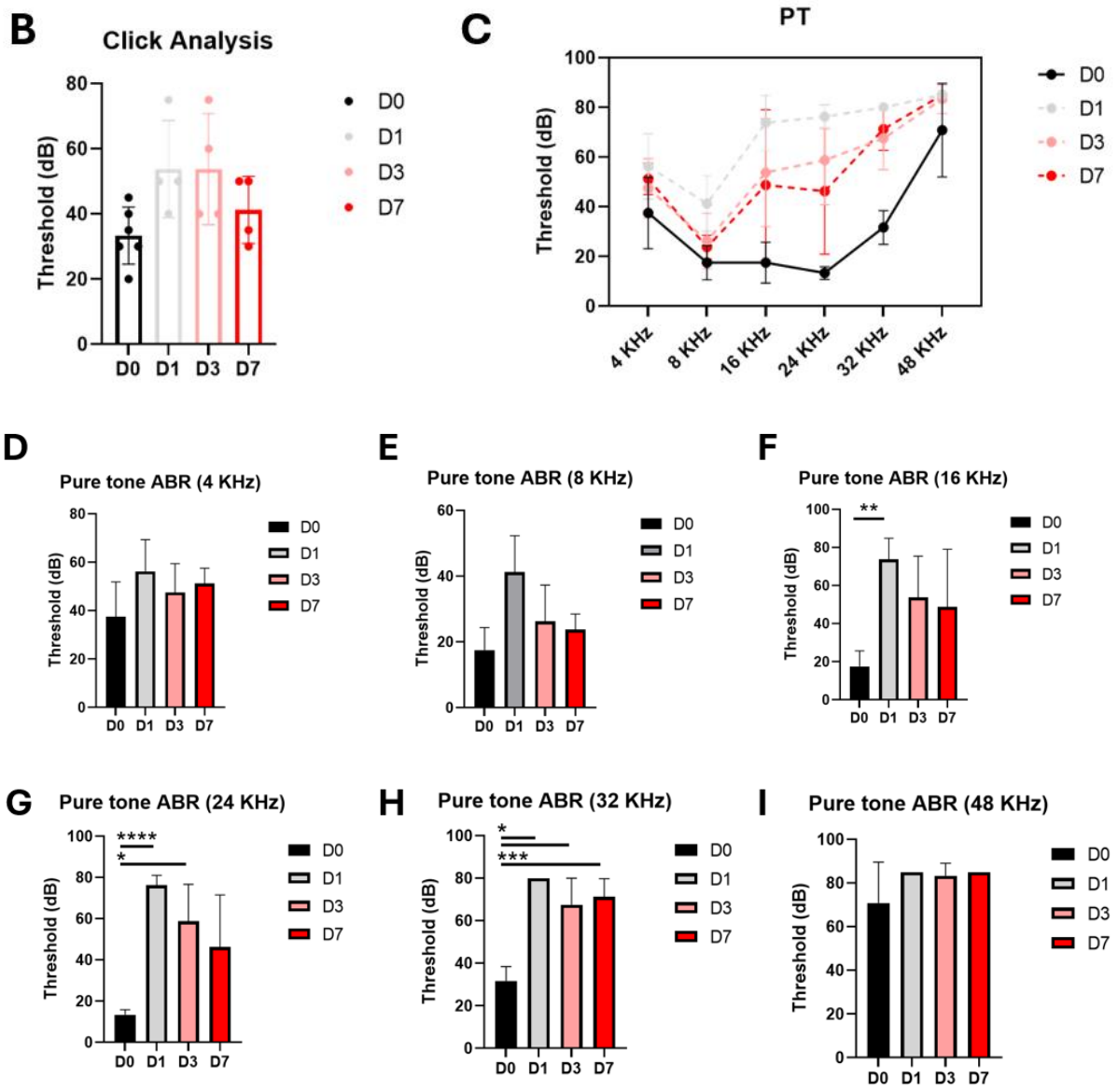

Figure 17. Effect of noise exposure on hearing thresholds of 6-week-old mice. A. Experimental Design. Six-week-old mice were exposed to sounds of 8-16 kHz for 2h at 100 dB and ABRs were recorded pre-exposure (D0), one day (D1), three days (D3) and seven days (D7) after trauma.

B. Click ABR thresholds, represented as mean +/- SD. Six mice were recorded at D0 while four mice were recorded on D1, D3 & D7. Mixed model ANOVA was performed (p-val = 0.051).

C. Pure tone ABR thresholds at all sound frequencies tested, represented as mean +/- SD. Six mice were recorded at D0 while four mice were recorded on D1, D3 & D7.

D-I. ABR thresholds for 4 kHz (D), 8 kHz (E), 16 kHz (F), 24 kHz (G), 32 kHz (H) and 48 kHz (I) sound frequencies, represented as mean +/- SD. Six mice were recorded at D0 while four mice were recorded at D1, D3 & D7. Mixed model ANOVA was performed (pval = 0,005) and Dunnett's multiple comparison test was performed as post hoc analysis. * = pval < 0,05, ** = pval < 0,01, *** = pval < 0,001 & **** = pval < 0,0001.

B. Effect of noise exposure on microglial activation in six-week-old mice.

Depending on sound intensity and duration, noise exposure has also been reported by several studies to induce inflammation inside the cochlea, leading to the recruitment of immune cells and microglial activation (Warchol 2019). Inflammation can either be helpful by helping clean debris and enhance regeneration or detrimental, particularly if it damages HCs or other important cochlear structures. To confirm our noise exposure model and verify whether inflammation occurred, we aimed at verifying the presence of IBA1-positive cells, a known microglia activation marker. Hence, we stained cochlear sections for IBA1 in six-week-old mice in the whole cochlea and at the middle turn. At D0 before noise exposure, we can see a weak background signal for IBA1 across the tissue (Figure 18), however strongly stained IBA1-positive microglial cells could occasionally be observed, mainly in the spiral ligament (not shown). Following noise exposure, especially from D1 to D5, we can see a notable increase in the number of IBA1-positive cells in the spiral ganglion, limbus, ligament and in the organ of Corti (red arrows). One week following trauma, microglial cells were still visible in the spiral ligament and limbus, however their number seemed to decrease compared to D3 and D5, especially in the organ of Corti. Although quantifications of microglial cells should be performed on more samples, our immunostaining results suggest that noise exposure indeed induces inflammation and microglial activation in the inner ear, confirming our noise exposure model.

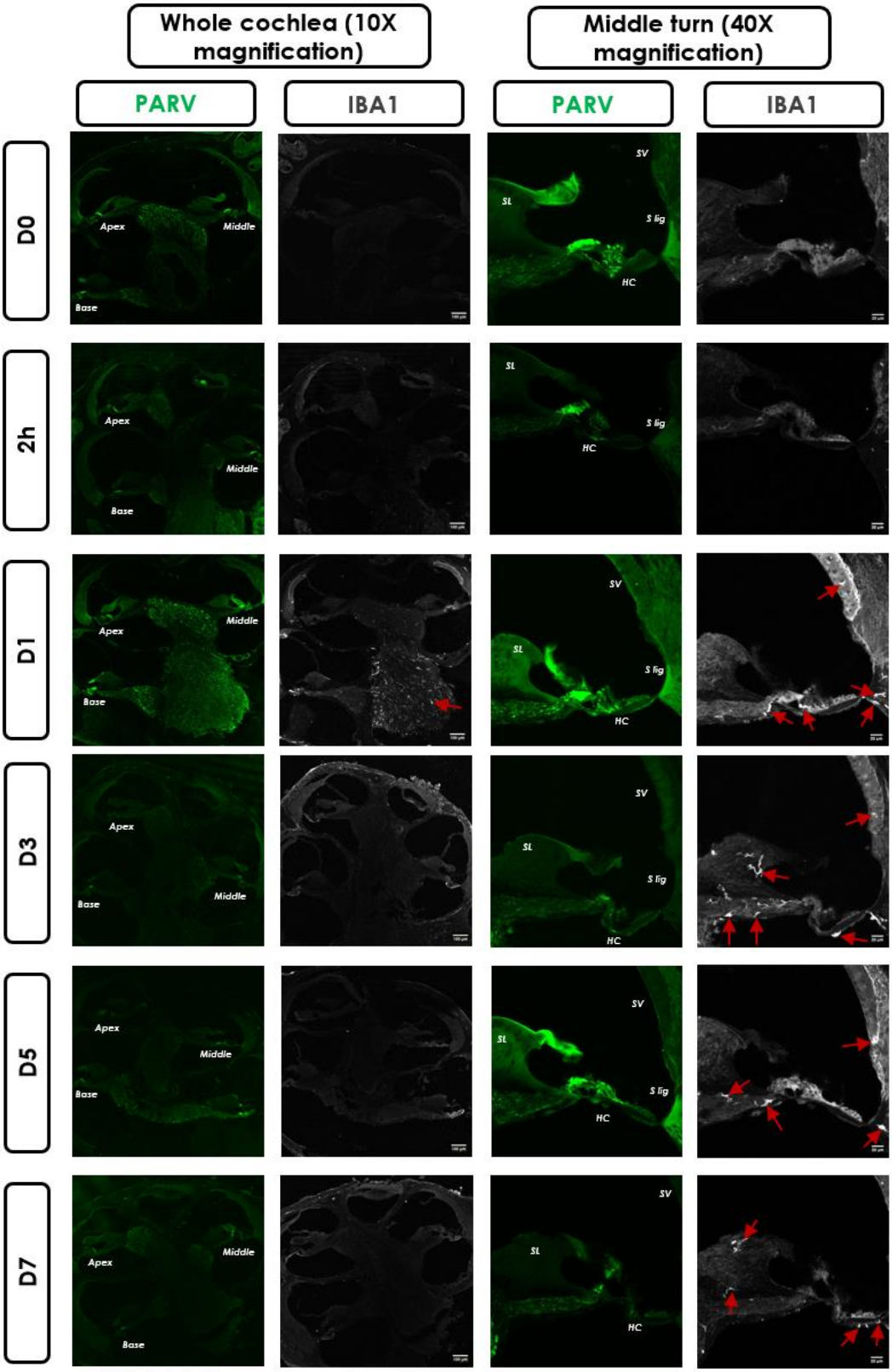

Figure 18. Effect of noise exposure on cochlear inflammation as evidenced by the presence of IBA1-positive microglial cells of six-week-old mice.

Cochlear sections were immunostained for IBA1 (white) to label microglial cells and for PARV (green) to visualize the cochlear HCs and SGNs. Images were acquired at 10x magnification (whole cochlea, left panels) and 40x magnification (focusing on the organ of Corti at the middle

turn, right panels) from mouse samples pre-exposure (D0), 2 hours (2h), one day (D1), three days (D3), five days (D5) and seven days (D7) after trauma.

C. Effect of noise exposure on MMPs localisation and expression level of six-week-old mice.

As inflammation has been reported to increase several MMPs' expression and activity (Li et al. 2015), we highly suspect that changes also occur following noise exposure. A previous study even showed MMP2 and MMP9 upregulation in the cochleae of noise traumatised mice, suggesting that these MMPs could play a key role in the modulation of ECM damage following noise exposure (Wu et al. 2017). Hence, we sought to investigate how noise exposure impacted MMPs expression levels as well as their distribution inside the cochlea.

First, we performed RT-qPCR to assess transcripts levels of the two gelatinases, MMP2 and MMP9 on 6-week-old wild type mice at different timepoints following trauma. Three mice were analysed for each group, except for our control condition (pre-exposure), for which high quality RNA could only be extracted for one mouse. This is highly unfortunate as one control sample is insufficient to draw conclusive results when comparing levels to the baseline expression levels. In Figure 19, we can see that MMP2 transcript levels slightly increases between 2h and D3 before going down progressively until D7, reaching similar levels than 2h after trauma. MMP9 level did not follow the same tendency as it seems to be decreased from D1 up to D7. We also checked IL6 as an inflammation marker and, as expected, IL6 transcript levels were strongly increased after noise exposure at all timepoints. Altogether, these results suggest that MMP2 and MMP9 are both differentially expressed after noise exposure which could hint at a potential role in ECM remodelling during noise exposure. We should however keep in mind that none of these results are significant, and conclusions could only be drawn after increasing the number of samples analysed per groups.

Next, we performed immunofluorescence on mice at the same timepoints, staining not only for MMP2 and MMP9 but also for one of their most well-known substrates, collagen 4 (COL 4). These timepoints were 2 hours after (2h), one day after (D1), three days after (D3), five days after (D5), seven days after (D7) trauma as well as our control, before trauma (D0). In the pre-exposure condition, we detected low levels of MMP2 protein everywhere in the cochlea and high levels in the otic capsule surrounding the tissue (Figure 20, left panel D0). Conveniently, type 4 collagen seems to be absent from the compartments where MMP2 is enriched and present in all the others. MMP9 protein seems to be specifically present in the organ of Corti and inside the TM (Figure 20, left and right panels D0). After noise exposure, we can see that MMP2 staining is strongly increased in the whole cochlear tissue, particularly in the otic capsule and in boundary regions

with fluidic compartments (Figure 20, left panels). At higher magnification, we can see MMP2 is upregulated in the spiral ligament and along the auditory nerve fibres from 2h to D5, before returning to lower levels at D7 (Figure 20, right panels). In contrast, MMP9 levels do not seem globally elevated in the whole cochlea following noise trauma (Figure 20, left panels) however, protein content could be progressively higher in the spiral ligament as the MMP9 staining seems stronger in this region at D3, D5 and D7.

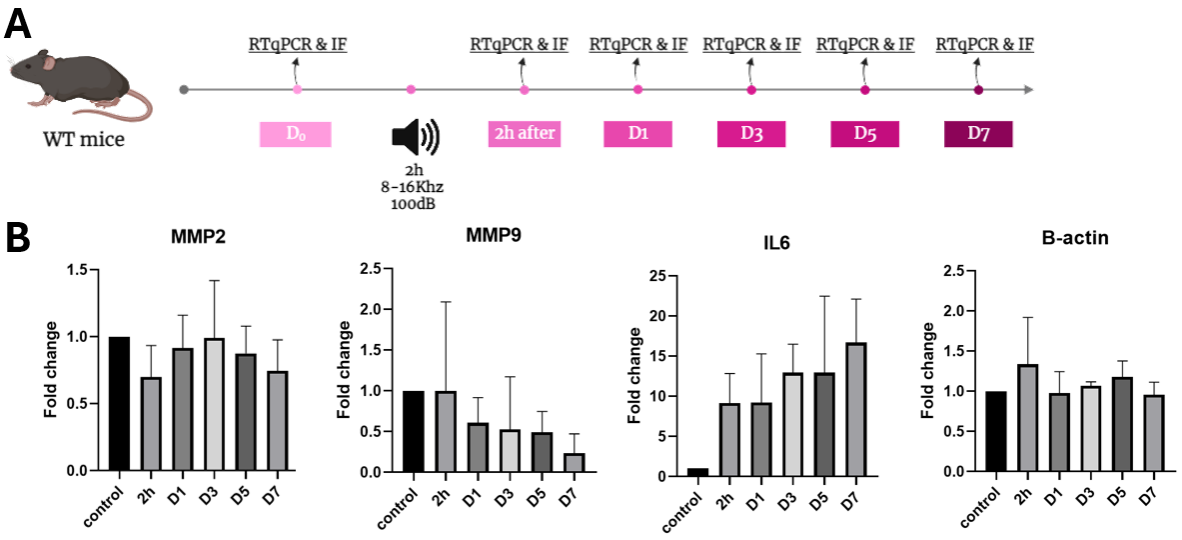

Figure 19. Effect of noise exposure on MMP2 and MMP9 transcript levels of six-week-old mice.

A. Timeline of the cochlear extractions following trauma for RT-qPCRs and Immunofluorescence.

B. RT-qPCR was performed on MMP2, MMP9, IL6 and B-Actin mRNA extracted from mice before sound exposure (D0), 2 hours (2h), one day (D1), three days (D3), five days (D5) and seven days (D7) after trauma. The mRNA levels were normalized on that of 36B4, and the results are shown relative to the normalized levels of pre-exposed mice (n=3 mice per time points, except for the control condition where n=1). Data are shown as mean +/- SD on which ANOVA has been performed (pval > 0,05).

Again, this experiment should be repeated on additional samples to conclude on MMP2 and MMP9 protein levels in the whole cochlea and in particular compartments following noise exposure. However, our results point out towards some interesting changes in protein abundance that demand further analyses.

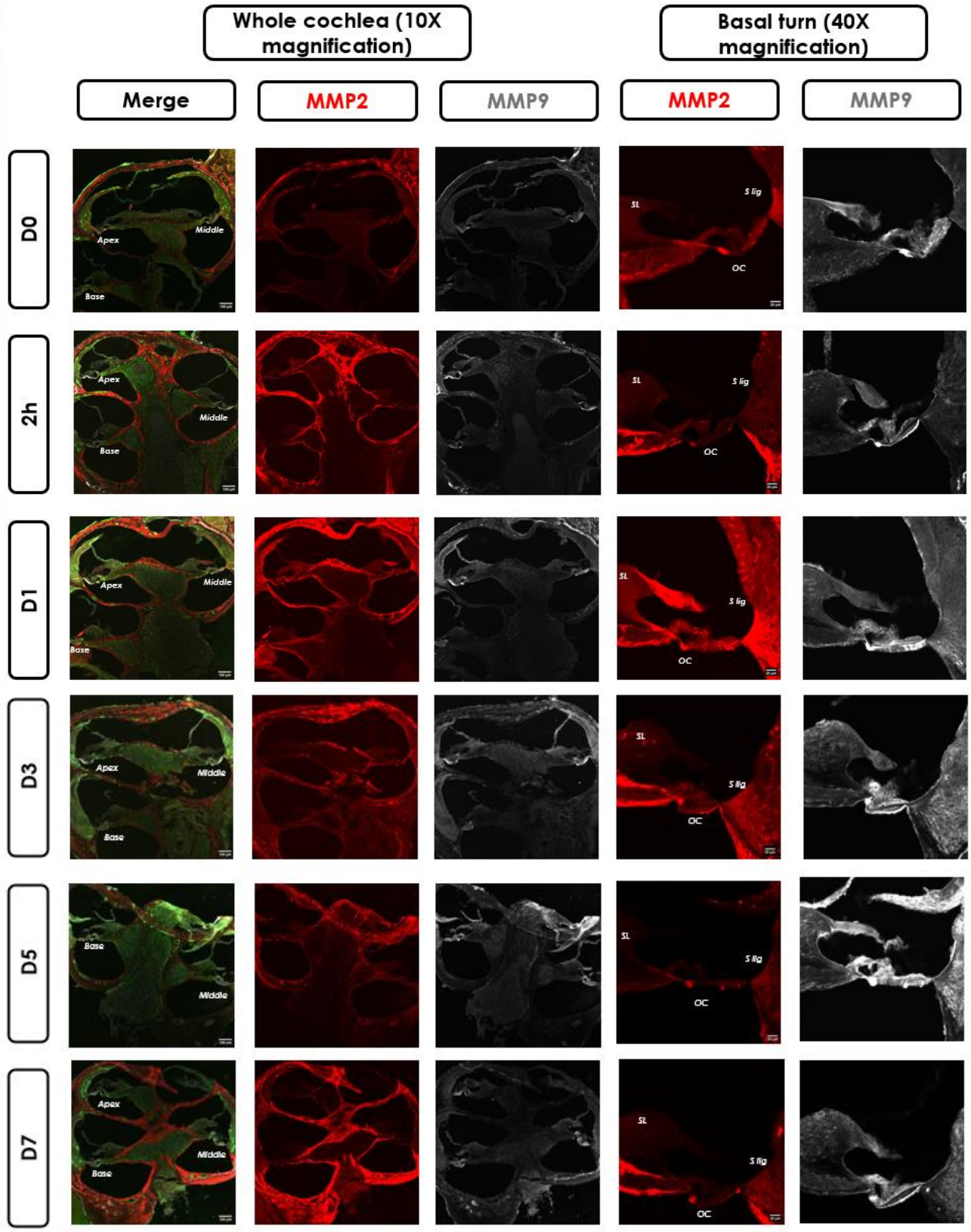

Figure 20. Effect of noise exposure on MMP2 and MMP9 localisation in six-week-old mice.

COL4, MMP2 and MMP9 immunostainings of cochlear sections at 10x magnification (whole cochlea) and at 40x magnification, focusing on the organ of corti at the basal turn, from mice pre-exposure (D0), 2 hours (2h), one day (D1), three days (D3), five days (D5) and seven days (D7) after trauma.

Discussion

In humans, the ECM is essential to the hearing function, with many gene mutations and proteins suspected to play key roles in cochlear dynamics. Nevertheless, it remains unclear what the roles of certain ECM regulators are, despite strong association with disease. Hence, we decided to investigate three of these, CEMIP, a hyaluronidase, and the gelatinases MMP2 and MMP9. For CEMIP study and the regulation of HA levels in the cochlea, we have shown the presence of key synthases, namely HAS2 and HAS3, during development in the forming spiral limbus and spiral ganglion neurons. In addition, we assessed the hearing function of Cemip-deficient mice at different ages. Our results indicate that, up to 16 weeks of age, Cemip seems dispensable for hearing as the gene invalidation had no impact on the hearing threshold of mice. For the second part of the project, namely MMPs, we demonstrated a clear hearing loss and inflammatory response in the cochleae of mice exposed to noise. RT-qPCR data suggest that noise induces a transient upregulation of MMP2 gelatinase and a progressive reduction of MMP9, at the transcriptional level. Immunostainings confirm the upregulation of MMP2 enzyme in many ECM compartments of the traumatized cochlea, including the otic capsule and the spiral ligament. However, we did not observe a decrease in MMP9 protein levels, but rather evidenced its local upregulation in the organ of Corti and spiral ligament following noise trauma. We believe that MMP2 and MMP9 expression changes could serve time-specific functions following sound overexposure, depending on their respective dynamics and cochlear locations.

HAS2 and Cemip regulate HA content around HCs

Previous RT-qPCR and RNAscope results obtained in our lab indicated the presence of HAS2 and HAS3 and the absence of HAS1 in the cochlea during embryonic stages and postnatal development up to P7. Our RNAscope assay clearly recapitulates those results, as we confirmed HAS 2 and HAS 3 expression in the cochlea at birth but were unable to detect HAS1 transcript. In addition, we also show that it is still the case at P15, when hearing is functional, although signal is weaker. Our results indicate that these two synthases are probably the main HA synthesizing enzymes for the cochlear ECM. Importantly, the regions in which both are enriched only modestly overlap, as HAS2 is mainly located around HCs and in the spiral limbus and HAS3 in the SGNs. This suggests that their activity is not redundant. At these stages, Cemip expression is high around the HCs, where HAS2 is enriched. It is thus possible that HA content, in this specific area of the cochlea, is under the control of HAS2 and Cemip opposite activities. As HAS2 is known to synthesize large-sized HA polymers, Cemip action would be necessary for its degradation into smaller fragments or even its elimination (Itano et al. 1999). Indeed, the absence of Cemip

hyaluronidase leads to the ectopic accumulation of HA in this precise cochlear region (see introduction, Figure 9).

Is Cemip truly a deafness-causing gene?

Although a study reported invalidating cemip gene mutations in patients suffering from hearing loss (Abe, Usami, and Nakamura 2003), we observed no hearing decline in Cemip-deficient mice up to 16 weeks of age. Before concluding that Cemip-induced degradation of HA is not required to preserve audition along the lifetime, more work is needed. First, our ABR recordings could be further analysed to check for more subtle defects than hearing threshold elevation. The loss of auditory synapses between IHC and SGNs can affect the hearing function without inducing a threshold shift, but rather manifests by a decreased amplitude of the first peak recorded in ABR (Liberman and Kujawa 2017). Indeed, this electrical response corresponds to cochlear nerve activity (see Figure 15A), therefore it would be reduced upon synaptopathy, which disrupts the communication between IHC and afferent SGNs. Hence, peak 1 amplitude should be measured in our 8 weeks old and 16 weeks old mice. If a difference is observed between WT and Cemip KO mice, some of them could be sacrificed to quantify the number of auditory synapses present at the basal pole of IHCs. Synaptic loss is the first cochlear damage that occurs with ageing, long before HC death (Sergeyenko et al. 2013). It is generally followed by neurite retraction, which correlates with long term consequences on SGN survival as they are no longer provided with trophic factors from their target cells. Ultimately, synaptopathies thus lead to SGN degeneration and hearing decline. As such, if we measure a decreased cochlear nerve activity and a loss of auditory synapses in 16-weeks-old Cemip KO mice, it is expected that older mice will present accelerated or exacerbated age-related hearing loss compared to WT littermates. This will be tested in the near future since our longitudinal study of their hearing function is ongoing. Investigating these key subsequent time points could thus help us definitively conclude on the role of Cemip in mice.

Importantly, the human Cemip study by Abe et al. reported genetic mutations in congenital and prelingual cases of deafness (Abe, Usami, and Nakamura 2003). This contrasts with our study of Cemip-deficient mice as their hearing sensitivity is unaffected in young and adult animals and raises questions concerning the relevance of the mouse model. This would not be an exception, as other diseases, including syndromic hearing loss, have failed to be recapitulated in mouse. The Alport mouse model, for instance, harbouring mutations in Col4 gene and displaying abnormalities in the ECM surrounding cochlear capillaries, have a normal hearing function (Cosgrove et al. 1998). These discrepancies between humans and mice are likely to arise from

anatomical and gene expression differences across species. Cemip expression pattern has not been investigated in human samples but studies in non-human primates reveal a more widespread profile in cochlea compared to mouse. Interestingly, a recent study reported the absence of a catalytic activity for Cemip2 hyaluronidase in humans (Sato et al. 2023). This important difference in catabolic activity could explain how, in mouse, Cemip loss could be compensated by another hyaluronidase, while its absence in humans leads to hearing loss. Finally, it is important to mention that Abe's study is only correlative as no causative effect has been demonstrated to refer Cemip as a deafness-causing gene in humans. Moreover, Cemip mutations were discovered in only 2 families in 2003 and no further studies have reported an association between Cemip genetic variations and deafness until now.

Noise-induced hearing loss mouse model

By analysing mice hearing thresholds after being exposed to sounds of 100 dB at 8 to 16 kHz for 2 hours, we measured a clear increase in ABR thresholds from day one to day seven. This augmentation is the result of noise induced damage, which can target many structures. The most obvious target of this damage are the hair cells which have been shown to be targeted at multiple levels. First, the hair cells' stereocilia can be affected by noise exposure leading to their fusion, collapse, detachment or even loss. The plasma membrane can also be affected, on one hand by mechanical stress leading to stretching injury of the membrane and on the other hand by metabolic stress eventually leading to lipid peroxidation which permeabilizes the membrane (Hu 2012). Apoptosis and necrosis of the hair cells can also be triggered by noise exposure, causing the loss of entire hair cells at the lesion site. Noise exposure can also affect the synapses formed by the hair cells and the peripheral projections of the spiral ganglion neurons

Our protocol, which is rather mild compared to others found in literature, seems to induce transient hearing loss at 8, 16 and 24 kHz, since the hearing thresholds were at least partially restored at D7. In contrast, hearing loss at 32 kHz is likely to be permanent as hearing sensitivity did not recover, even one week after noise trauma. To definitively conclude on the transient versus permanent feature of hearing loss, functional tests should have been performed up to 21 days, however we can already make some assumptions regarding the actual importance of the lesion in different tonotopic regions of the inner ear. For instance, HC loss could only occur for cochlear regions that do not recover from noise trauma, such as the 32 kHz-sensitive area located at the basal turn of the cochlea. Indeed, HC loss cannot be functionally compensated and would irremediably result in a permanent decrease in sound detection. A study conducted by Erlandsson (1980) demonstrated that sound intensity dictates the number of lost hair cells

although it was necessary to reach a certain threshold to observe significant hair cell loss. Indeed, after exposing guinea pigs to sound intensities of 102 to 117 dB SPL, the number of missing OHCs rose from 5 to 8%. However, after reaching 120 dB SPL, the number of missing OHCs rose to 37%, indicating that hair cell loss is non-linear. It is likely that these critical sound intensities have not been reached in our experiment and that most of the noise-induced damage occurring in our model relates to stereocilia defects or synapse disruption, which can both be reversible. Interestingly, these structures rely on exquisite cochlear ECM types, as stereocilia are anchored and protected by the TM and synapses are ensheathed by the PNNs to ensure their stabilisation. The transient feature of hearing loss we evidenced at 16 and 24 kHz, could thus reflect ECM breakdown immediately after noise exposure, followed by extensive ECM remodelling to repair the protective structures around stereocilia and synapses. To further characterize our model, scanning electron microscopy could be conducted on surface preparations of cochleae to evaluate the integrity of the hair bundle responsible for sound detection. In parallel, confocal microscopy would be useful to monitor the spatial coupling of pre- and post-synaptic machineries (labelled by Ribeye and GluR2, respectively) at different timepoints following noise exposure.

By analysing microglial cells through immunostaining and pro-inflammatory cytokine IL6 levels by RT-PCR, we confirmed inflammation does indeed occur in our noise exposure model. Inflammation is a key process as previous studies have shown that the recruitment of macrophages and activation of resident cells can either be helpful or detrimental to regeneration (Warchol 2019). In general, these studies are performed by exposing their mice to more severe trauma, going up to 120 dB over the course of 4 hours and observing ameboid cells populating the spiral ganglion, limbus, ligament and lateral wall of the scala media. Depending on the duration and intensity of exposure, the type of damage appearing will largely differ. In our case, 100 dB was enough to elicit microglial activation in the spiral ligament, the BM as well as the spiral limbus for up to seven days following noise. Further studies on additional samples, including cell quantifications, histological analysis of the microglia morphology and specific markers, could be helpful to characterise the extent and nature of cochlear inflammation. Moreover, flow cytometry could help us determine the polarisation of microglia and identify M1-like immune cells, that generally contribute to damage inside the tissue, and M2-like immune cells, which designates the phenotype that helps tissue regeneration and neuroprotection.

MMP expression changes after noise exposure

By investigating MMP2 and MMP9 transcript levels and protein distribution, we assessed their evolution in the cochlea after trauma. For MMP2, RT-qPCR results showed a transient and modest increase in transcript levels after exposure, while MMP9 tended to decrease in the same conditions. These results are very surprising as they are in disagreement with previously published results that showed a net increase in both MMP levels through proteomics analysis of mice exposed to 120 dB for 4h (Wu et al. 2017). This could result from the lack of a sufficient number of control animals in our experiments, as one of them died over the course of the experiment and poor-quality RNA was extracted from a second one. As such, statistical analysis of the variations between the different timepoints and baseline levels were impossible to conduct, and data are thus difficult to interpret. Increasing the number of animals in the control condition could be a first way of increasing the reliability of our results. Besides, discrepancies can also be explained by differences in experimental designs, as we have exposed the mice to only 100 dB. As the decibel scale is logarithmic, this 20 dB difference is far from being anecdotic.

Immunostainings, on mice exposed to noise in identical circumstances, revealed the upregulation of both these MMPs in different cochlear compartments. MMP9 was mainly increased in the HC region and in the spiral limbus and ligament, while MMP2 seemed to be drastically increased in the otic capsule and TM. These results are consistent with those obtained in similar studies, however, it is hard to draw any robust conclusions as only one animal was used per timepoint. The discrepancies between our RT-qPCR data and immunofluorescence data are also intriguing but could be explained by the fact that these techniques analyse different levels of gene expression as they detect RNA and protein, respectively. We cannot rule out that transcription rate and protein content are differentially regulated in cells and that their respective levels do not correlate. For instance, protein translation and stability could be increased following trauma although the messenger RNA is less produced. We must also keep in mind that, for RT-qPCRs, as we collected the entire cochleae (with otic capsule, modiolus and organ of Corti), the RNA we extracted is a mix of all these different cochlear compartments whereas immunostainings, which are poorly quantitative, allow the visualization of specific cochlear locations and we have only focused on the scala media region. Finally, it should be noted that we only checked for the presence of MMPs, whether they are in their active form or not. As there are many regulators of MMPs, among which, TIMP2 and TIMP3 can inhibit all existing MMPs, the activity of MMP2 and MMP9 should also be addressed. To do so, we could perform a zymography gel, which allows to see if the protein extracted are able to digest their gelatine substrates.

References

Abatangelo, G., V. Vindigni, G. Avruscio, L. Pandis, and P. Brun. 2020. 'Hyaluronic Acid: Redefining Its Role'. *Cells* 9 (7): 1743. https://doi.org/10.3390/cells9071743.

Abe, Satoko, Shin-ichi Usami, and Yusuke Nakamura. 2003. 'Mutations in the Gene Encoding KIAA1199 Protein, an Inner-Ear Protein Expressed in Deiters' Cells and the Fibrocytes, as the Cause of Nonsyndromic Hearing Loss'. *Journal of Human Genetics* 48 (11): 564–70. https://doi.org/10.1007/s10038-003-0079-2.

Anastasiadou, Sofia, and Yasir Al Khalili. 2024. 'Hearing Loss'. In *StatPearls*. Treasure Island (FL): StatPearls Publishing. http://www.ncbi.nlm.nih.gov/books/NBK542323/.

Appler, Jessica M., and Lisa V. Goodrich. 2011. 'Connecting the Ear to the Brain: Molecular Mechanisms of Auditory Circuit Assembly'. *Progress in Neurobiology* 93 (4): 488–508. https://doi.org/10.1016/j.pneurobio.2011.01.004.

Bart, Geneviève, Nuria Ortega Vico, Antti Hassinen, Francois M. Pujol, Ashik Jawahar Deen, Aino Ruusala, Raija H. Tammi, et al. 2015. 'Fluorescence Resonance Energy Transfer (FRET) and Proximity Ligation Assays Reveal Functionally Relevant Homo- and Heteromeric Complexes among Hyaluronan Synthases HAS1, HAS2, and HAS3'. *The Journal of Biological Chemistry* 290 (18): 11479–90. https://doi.org/10.1074/jbc.M115.640581.

Bonnans, Caroline, Jonathan Chou, and Zena Werb. 2014. 'Remodelling the Extracellular Matrix in Development and Disease'. *Nature Reviews. Molecular Cell Biology* 15 (12): 786–801. https://doi.org/10.1038/nrm3904.

Buckiova, Daniela, Jiri Popelar, and Josef Syka. 2006. 'Collagen Changes in the Cochlea of Aged Fischer 344 Rats'. *Experimental Gerontology* 41 (3): 296–302. https://doi.org/10.1016/j.exger.2005.11.010.

Caprara, Giusy A., and Anthony W. Peng. 2022. 'Mechanotransduction in Mammalian Sensory Hair Cells'. *Molecular and Cellular Neurosciences* 120 (May):103706. https://doi.org/10.1016/j.mcn.2022.103706.

Cohen, Roie, and David Sprinzak. 2021. 'Mechanical Forces Shaping the Development of the Inner Ear'. *Biophysical Journal* 120 (19): 4142–48. https://doi.org/10.1016/j.bpj.2021.06.036.

Cosgrove, D., G. Samuelson, D. T. Meehan, C. Miller, J. McGee, E. J. Walsh, and M. Siegel. 1998. 'Ultrastructural, Physiological, and Molecular Defects in the Inner Ear of a Gene-Knockout

Mouse Model for Autosomal Alport Syndrome'. *Hearing Research* 121 (1–2): 84–98. https://doi.org/10.1016/s0378-5955(98)00069-0.

Dufek, Brianna, Daniel T. Meehan, Duane Delimont, Gina Samuelson, Jacob Madison, Xiourui Shi, Flint Boettcher, Vincent Trosky, Michael Anne Gratton, and Dominic Cosgrove. 2020. 'Pericyte Abnormalities Precede Strial Capillary Basement Membrane Thickening in Alport Mice'. *Hearing Research* 390 (May):107935. https://doi.org/10.1016/j.heares.2020.107935.

Fettiplace, Robert. 2023. 'Cochlear Tonotopy from Proteins to Perception'. *BioEssays: News and Reviews in Molecular, Cellular and Developmental Biology* 45 (8): e2300058. https://doi.org/10.1002/bies.202300058.

Frantz, Christian, Kathleen M. Stewart, and Valerie M. Weaver. 2010. 'The Extracellular Matrix at a Glance'. *Journal of Cell Science* 123 (Pt 24): 4195–4200. https://doi.org/10.1242/jcs.023820.

Fuchs, Paul Albert, and Amanda M. Lauer. 2019. 'Efferent Inhibition of the Cochlea'. *Cold Spring Harbor Perspectives in Medicine* 9 (5): a033530. https://doi.org/10.1101/cshperspect.a033530.

Gavara, Núria, and Richard S. Chadwick. 2009. 'Collagen-Based Mechanical Anisotropy of the Tectorial Membrane: Implications for Inter-Row Coupling of Outer Hair Cell Bundles'. *PloS One* 4 (3): e4877. https://doi.org/10.1371/journal.pone.0004877.

Goodyear, Richard J., Xiaowei Lu, Michael R. Deans, and Guy P. Richardson. 2017. 'A Tectorin-Based Matrix and Planar Cell Polarity Genes Are Required for Normal Collagen-Fibril Orientation in the Developing Tectorial Membrane'. *Development (Cambridge, England)* 144 (21): 3978–89. https://doi.org/10.1242/dev.151696.

Goodyear, Richard J., and Guy P. Richardson. 2018. 'Structure, Function, and Development of the Tectorial Membrane: An Extracellular Matrix Essential for Hearing'. *Current Topics in Developmental Biology* 130:217–44. https://doi.org/10.1016/bs.ctdb.2018.02.006.

Gratton, Michael Anne, Velidi H. Rao, Daniel T. Meehan, Charles Askew, and Dominic Cosgrove. 2005. 'Matrix Metalloproteinase Dysregulation in the Stria Vascularis of Mice with Alport Syndrome: Implications for Capillary Basement Membrane Pathology'. *The American Journal of Pathology* 166 (5): 1465–74. https://doi.org/10.1016/S0002-9440(10)62363-2.

Hashizume, Misato, and Masahiko Mihara. 2010. 'High Molecular Weight Hyaluronic Acid Inhibits IL-6-Induced MMP Production from Human Chondrocytes by up-Regulating the ERK Inhibitor, MKP-1'. *Biochemical and Biophysical Research Communications* 403 (2): 184–89. https://doi.org/10.1016/j.bbrc.2010.10.135.

Heine, Patricia A. 2004. ‘Anatomy of the Ear’. *The Veterinary Clinics of North America. Small Animal Practice* 34 (2): 379–95. https://doi.org/10.1016/j.cvsm.2003.10.003.

Hu, Bohua. 2012. ‘Noise-Induced Structural Damage to the Cochlea’. In *Noise-Induced Hearing Loss: Scientific Advances*, edited by Colleen G. Le Prell, Donald Henderson, Richard R. Fay, and Arthur N. Popper, 57–86. New York, NY: Springer. https://doi.org/10.1007/978-1-4419-9523-0_5.

Ishiyama, Akira, Sarah E. Mowry, Ivan A. Lopez, and Gail Ishiyama. 2009. ‘Immunohistochemical Distribution of Basement Membrane Proteins in the Human Inner Ear from Older Subjects’. *Hearing Research* 254 (1–2): 1–14. https://doi.org/10.1016/j.heares.2009.03.014.

Itano, N., T. Sawai, M. Yoshida, P. Lenas, Y. Yamada, M. Imagawa, T. Shinomura, et al. 1999. ‘Three Isoforms of Mammalian Hyaluronan Synthases Have Distinct Enzymatic Properties’. *The Journal of Biological Chemistry* 274 (35): 25085–92. https://doi.org/10.1074/jbc.274.35.25085.

Jean, Philippe, Fabienne Wong Jun Tai, Amrit Singh-Estivalet, Andrea Lelli, Cyril Scandola, Sébastien Megharba, Sandrine Schmutz, et al. 2023. ‘Single-Cell Transcriptomic Profiling of the Mouse Cochlea: An Atlas for Targeted Therapies’. *Proceedings of the National Academy of Sciences of the United States of America* 120 (26): e2221744120. https://doi.org/10.1073/pnas.2221744120.

Jeng, Jing-Yi, Csaba Harasztosi, Adam J. Carlton, Laura F. Corns, Philine Marchetta, Stuart L. Johnson, Richard J. Goodyear, et al. 2021. ‘MET Currents and Otoacoustic Emissions from Mice with a Detached Tectorial Membrane Indicate the Extracellular Matrix Regulates Ca2+ near Stereocilia’. *The Journal of Physiology* 599 (7): 2015–36. https://doi.org/10.1113/JP280905.

Jongkamonwiwat, Nopporn, Miguel A. Ramirez, Seby Edassery, Ann C. Y. Wong, Jintao Yu, Tirzah Abbott, Kwang Pak, Allen F. Ryan, and Jeffrey N. Savas. 2020. ‘Noise Exposures Causing Hearing Loss Generate Proteotoxic Stress and Activate the Proteostasis Network’. *Cell Reports* 33 (8): 108431. https://doi.org/10.1016/j.celrep.2020.108431.

Kim, Hyebin, Junghwa Cha, Minjeong Jang, and Pilnam Kim. 2019. ‘Hyaluronic Acid-Based Extracellular Matrix Triggers Spontaneous M2-like Polarity of Monocyte/Macrophage’. *Biomaterials Science* 7 (6): 2264–71. https://doi.org/10.1039/c9bm00155g.

Kim, Kyunghee X., Joel D. Sanneman, Hyoung-Mi Kim, Donald G. Harbidge, Jie Xu, Manoocher Soleimani, Philine Wangemann, and Daniel C. Marcus. 2014. ‘Slc26a7 Chloride Channel Activity and Localization in Mouse Reissner’s Membrane Epithelium’. *PloS One* 9 (5): e97191. https://doi.org/10.1371/journal.pone.0097191.

Kobayashi, Takashi, Theerawut Chanmee, and Naoki Itano. 2020. 'Hyaluronan: Metabolism and Function'. *Biomolecules* 10 (11): 1525. https://doi.org/10.3390/biom10111525.

Kundu, Soumi, Neetu Tyagi, Utpal Sen, and Suresh C. Tyagi. 2009. 'Matrix Imbalance by Inducing Expression of Metalloproteinase and Oxidative Stress in Cochlea of Hyperhomocysteinemic Mice'. *Molecular and Cellular Biochemistry* 332 (1–2): 215–24. https://doi.org/10.1007/s11010-009-0194-2.

Landin Malt, Andre, Zachary Dailey, Julia Holbrook-Rasmussen, Yuqiong Zheng, Arielle Hogan, Quansheng Du, and Xiaowei Lu. 2019. 'Par3 Is Essential for the Establishment of Planar Cell Polarity of Inner Ear Hair Cells'. *Proceedings of the National Academy of Sciences of the United States of America* 116 (11): 4999–5008. https://doi.org/10.1073/pnas.1816333116.

Lee-Thedieck, Cornelia, Peter Schertl, and Gerd Klein. 2022. 'The Extracellular Matrix of Hematopoietic Stem Cell Niches'. *Advanced Drug Delivery Reviews* 181 (February):114069. https://doi.org/10.1016/j.addr.2021.114069.

Li, Wu-Li, Cheng-Hai Wu, Jun Yang, Min Tang, Long-Jie Chen, and Shou-Liang Zhao. 2015. 'Local Inflammation Alters MMP-2 and MMP-9 Gelatinase Expression Associated with the Severity of Nifedipine-Induced Gingival Overgrowth: A Rat Model Study'. *Inflammation* 38 (4): 1517–28. https://doi.org/10.1007/s10753-015-0126-0.

Liberman, M. Charles, and Sharon G. Kujawa. 2017. 'Cochlear Synaptopathy in Acquired Sensorineural Hearing Loss: Manifestations and Mechanisms'. *Hearing Research* 349 (June):138–47. https://doi.org/10.1016/j.heares.2017.01.003.

Liu, Wei, Francesca Atturo, Robair Aldaya, Peter Santi, Sebahattin Cureoglu, Sabrina Obwegeser, Rudolf Glueckert, Kristian Pfaller, Annelies Schrott-Fischer, and Helge Rask-Andersen. 2015. 'Macromolecular Organization and Fine Structure of the Human Basilar Membrane - RELEVANCE for Cochlear Implantation'. *Cell and Tissue Research* 360 (2): 245–62. https://doi.org/10.1007/s00441-014-2098-z.

Liu, Wei, Åsa Johansson, Helge Rask-Andersen, and Mathias Rask-Andersen. 2021. 'A Combined Genome-Wide Association and Molecular Study of Age-Related Hearing Loss in H. Sapiens'. *BMC Medicine* 19 (1): 302. https://doi.org/10.1186/s12916-021-02169-0.

Machado, Vera, Mariana Morais, and Rui Medeiros. 2022. 'Hyaluronic Acid-Based Nanomaterials Applied to Cancer: Where Are We Now?' *Pharmaceutics* 14 (10): 2092. https://doi.org/10.3390/pharmaceutics14102092.

Milenkovic, Ivan, Ulrich Schiefer, Regina Ebenhoch, and Judith Ungewiss. 2020. '[Anatomy and physiology of the auditory pathway]'. *Der Ophthalmologe: Zeitschrift Der Deutschen Ophthalmologischen Gesellschaft* 117 (11): 1068–73. https://doi.org/10.1007/s00347-020-01070-0.

Mochizuki, T., H. H. Lemmink, M. Mariyama, C. Antignac, M. C. Gubler, Y. Pirson, C. Verellen-Dumoulin, B. Chan, C. H. Schröder, and H. J. Smeets. 1994. 'Identification of Mutations in the Alpha 3(IV) and Alpha 4(IV) Collagen Genes in Autosomal Recessive Alport Syndrome'. *Nature Genetics* 8 (1): 77–81. https://doi.org/10.1038/ng0994-77.

Muggenthaler, Martina M. A., Biswajit Chowdhury, S. Naimul Hasan, Harold E. Cross, Brian Mark, Gaurav V. Harlalka, Michael A. Patton, et al. 2017. 'Mutations in HYAL2, Encoding Hyaluronidase 2, Cause a Syndrome of Orofacial Clefting and Cor Triatriatum Sinister in Humans and Mice'. *PLoS Genetics* 13 (1): e1006470. https://doi.org/10.1371/journal.pgen.1006470.

Naz, S., F. Alasti, A. Mowjoodi, S. Riazuddin, M. H. Sanati, T. B. Friedman, A. J. Griffith, E. R. Wilcox, and S. Riazuddin. 2003. 'Distinctive Audiometric Profile Associated with DFNB21 Alleles of TECTA'. *Journal of Medical Genetics* 40 (5): 360–63. https://doi.org/10.1136/jmg.40.5.360.

Neuman, Manuela G., Radu M. Nanau, Loida Oruña-Sanchez, and Gabriel Coto. 2015. 'Hyaluronic Acid and Wound Healing'. *Journal of Pharmacy & Pharmaceutical Sciences: A Publication of the Canadian Society for Pharmaceutical Sciences, Societe Canadienne Des Sciences Pharmaceutiques* 18 (1): 53–60. https://doi.org/10.18433/j3k89d.

Nishio, Shin-Ya, Mitsuru Hattori, Hideaki Moteki, Keita Tsukada, Maiko Miyagawa, Takehiko Naito, Hidekane Yoshimura, et al. 2015. 'Gene Expression Profiles of the Cochlea and Vestibular Endorgans: Localization and Function of Genes Causing Deafness'. *The Annals of Otology, Rhinology, and Laryngology* 124 Suppl 1 (May):6S-48S. https://doi.org/10.1177/0003489415575549.

Pressé, Mary T., Brigitte Malgrange, and Laurence Delacroix. 2024. 'The Cochlear Matrisome: Importance in Hearing and Deafness'. *Matrix Biology: Journal of the International Society for Matrix Biology* 125 (January):40–58. https://doi.org/10.1016/j.matbio.2023.12.002.

Ren, Tianying, Wenxuan He, and David Kemp. 2016. 'Reticular Lamina and Basilar Membrane Vibrations in Living Mouse Cochleae'. *Proceedings of the National Academy of Sciences of the United States of America* 113 (35): 9910–15. https://doi.org/10.1073/pnas.1607428113.

Rilla, Kirsi, Hanna Siiskonen, Andrew P. Spicer, Juha M. T. Hyttinen, Markku I. Tammi, and Raija H. Tammi. 2005. 'Plasma Membrane Residence of Hyaluronan Synthase Is Coupled to Its Enzymatic Activity'. *The Journal of Biological Chemistry* 280 (36): 31890–97. https://doi.org/10.1074/jbc.M504736200.

Russell, Ian J., Victoria A. Lukashkina, Snezana Levic, Young-Wook Cho, Andrei N. Lukashkin, Lily Ng, and Douglas Forrest. 2020. 'Emilin 2 Promotes the Mechanical Gradient of the Cochlear Basilar Membrane and Resolution of Frequencies in Sound'. *Science Advances* 6 (24): eaba2634. https://doi.org/10.1126/sciadv.aba2634.

Sato, Shinya, Megumi Miyazaki, Shinji Fukuda, Yukiko Mizutani, Yoichi Mizukami, Shigeki Higashiyama, and Shintaro Inoue. 2023. 'Human TMEM2 Is Not a Catalytic Hyaluronidase, but a Regulator of Hyaluronan Metabolism via HYBID (KIAA1199/CEMIP) and HAS2 Expression'. *The Journal of Biological Chemistry* 299 (6): 104826. https://doi.org/10.1016/j.jbc.2023.104826.

Schaefer, Liliana, and Roland M. Schaefer. 2010. 'Proteoglycans: From Structural Compounds to Signaling Molecules'. *Cell and Tissue Research* 339 (1): 237–46. https://doi.org/10.1007/s00441-009-0821-y.

Schraders, Margit, Laura Ruiz-Palmero, Ersan Kalay, Jaap Oostrik, Francisco J. del Castillo, Orhan Sezgin, Andy J. Beynon, et al. 2012. 'Mutations of the Gene Encoding Otogelin Are a Cause of Autosomal-Recessive Nonsyndromic Moderate Hearing Impairment'. *American Journal of Human Genetics* 91 (5): 883–89. https://doi.org/10.1016/j.ajhg.2012.09.012.

Sergeyenko, Yevgeniya, Kumud Lall, M. Charles Liberman, and Sharon G. Kujawa. 2013. 'Age-Related Cochlear Synaptopathy: An Early-Onset Contributor to Auditory Functional Decline'. *The Journal of Neuroscience: The Official Journal of the Society for Neuroscience* 33 (34): 13686–94. https://doi.org/10.1523/JNEUROSCI.1783-13.2013.

Shave, Samantha, Christina Botti, and Kelvin Kwong. 2022. 'Congenital Sensorineural Hearing Loss'. *Pediatric Clinics of North America* 69 (2): 221–34. https://doi.org/10.1016/j.pcl.2021.12.006.

Shin, Jung-Bum, and Peter G. Gillespie. 2009. 'Unraveling Cadherin 23's Role in Development and Mechanotransduction'. *Proceedings of the National Academy of Sciences of the United States of America* 106 (13): 4959–60. https://doi.org/10.1073/pnas.0902008106.

Shiryaev, S. A., A. G. Remacle, V. S. Golubkov, S. Ingvarsen, A. Porse, N. Behrendt, P. Cieplak, and A. Y. Strongin. 2013. 'A Monoclonal Antibody Interferes with TIMP-2 Binding and

Incapacitates the MMP-2-Activating Function of Multifunctional, pro-Tumorigenic MMP-14/MT1–MMP'. *Oncogenesis* 2 (12): e80–e80. https://doi.org/10.1038/oncsis.2013.44.

Sonntag, Mandy, Maren Blosa, Sophie Schmidt, Katja Reimann, Kerstin Blum, Tobias Eckrich, Gudrun Seeger, et al. 2018. 'Synaptic Coupling of Inner Ear Sensory Cells Is Controlled by Brevican-Based Extracellular Matrix Baskets Resembling Perineuronal Nets'. *BMC Biology* 16 (1): 99. https://doi.org/10.1186/s12915-018-0566-8.

Spataro, Sofia, Concetta Guerra, Andrea Cavalli, Jacopo Sgrignani, Jonathan Sleeman, Lina Poulain, Andreas Boland, Leonardo Scapozza, Solange Moll, and Marco Prunotto. 2023. 'CEMIP (HYBID, KIAA1199): Structure, Function and Expression in Health and Disease'. *The FEBS Journal* 290 (16): 3946–62. https://doi.org/10.1111/febs.16600.

Strimbu, Clark Elliott, Sonal Prasad, Pierre Hakizimana, and Anders Fridberger. 2019. 'Control of Hearing Sensitivity by Tectorial Membrane Calcium'. *Proceedings of the National Academy of Sciences of the United States of America* 116 (12): 5756–64. https://doi.org/10.1073/pnas.1805223116.

Suzuki, Mitsuya, Takashi Sakamoto, Akinori Kashio, and Tatsuya Yamasoba. 2016. 'Age-Related Morphological Changes in the Basement Membrane in the Stria Vascularis of C57BL/6 Mice'. *European Archives of Oto-Rhino-Laryngology: Official Journal of the European Federation of Oto-Rhino-Laryngological Societies (EUFOS): Affiliated with the German Society for Oto-Rhino-Laryngology - Head and Neck Surgery* 273 (1): 57–62. https://doi.org/10.1007/s00405-014-3478-4.

Tsuprun, V., and P. Santi. 2001. 'Proteoglycan Arrays in the Cochlear Basement Membrane'. *Hearing Research* 157 (1–2): 65–76. https://doi.org/10.1016/s0378-5955(01)00278-7.

Verpy, E., S. Masmoudi, I. Zwaenepoel, M. Leibovici, T. P. Hutchin, I. Del Castillo, S. Nouaille, et al. 2001. 'Mutations in a New Gene Encoding a Protein of the Hair Bundle Cause Non-Syndromic Deafness at the DFNB16 Locus'. *Nature Genetics* 29 (3): 345–49. https://doi.org/10.1038/ng726.

Wan, Guoqiang, Gabriel Corfas, and Jennifer S. Stone. 2013. 'Inner Ear Supporting Cells: Rethinking the Silent Majority'. *Seminars in Cell & Developmental Biology* 24 (5): 448–59. https://doi.org/10.1016/j.semcdb.2013.03.009.

Warchol, Mark E. 2019. 'Interactions between Macrophages and the Sensory Cells of the Inner Ear'. *Cold Spring Harbor Perspectives in Medicine* 9 (6): a033555. https://doi.org/10.1101/cshperspect.a033555.

Wu, Jun, Weiju Han, Xingrui Chen, Weiwei Guo, Ke Liu, Ruoya Wang, Jishuai Zhang, and Na Sai. 2017. 'Matrix Metalloproteinase-2 and -9 Contribute to Functional Integrity and Noise-induced Damage to the Blood-Labyrinth-Barrier'. *Molecular Medicine Reports* 16 (2): 1731–38. https://doi.org/10.3892/mmr.2017.6784.

Xie, Zhifang, Xian-Hua Ma, Qiu-Fang Bai, Jie Tang, Jian-He Sun, Fei Jiang, Wei Guo, et al. 2023. 'ZBTB20 Is Essential for Cochlear Maturation and Hearing in Mice'. *Proceedings of the National Academy of Sciences of the United States of America* 120 (24): e2220867120. https://doi.org/10.1073/pnas.2220867120.

Yoshida, Hiroyuki, Aya Nagaoka, Ayumi Kusaka-Kikushima, Megumi Tobiishi, Keigo Kawabata, Tetsuya Sayo, Shingo Sakai, et al. 2013. 'KIAA1199, a Deafness Gene of Unknown Function, Is a New Hyaluronan Binding Protein Involved in Hyaluronan Depolymerization'. *Proceedings of the National Academy of Sciences of the United States of America* 110 (14): 5612–17. https://doi.org/10.1073/pnas.1215432110.

Yoshida, Hiroyuki, Aya Nagaoka, Sachiko Nakamura, Megumi Tobiishi, Yoshinori Sugiyama, and Shintaro Inoue. 2014. 'N-Terminal Signal Sequence Is Required for Cellular Trafficking and Hyaluronan-Depolymerization of KIAA1199'. *FEBS Letters* 588 (1): 111–16. https://doi.org/10.1016/j.febslet.2013.11.017.

Zhang, Peng-Zhi, Ya He, Xing-Wang Jiang, Fu-Quan Chen, Yang Chen, Tao Xue, Ke Zhou, et al. 2013. 'Up-Regulation of Stromal Cell-Derived Factor-1 Enhances Migration of Transplanted Neural Stem Cells to Injury Region Following Degeneration of Spiral Ganglion Neurons in the Adult Rat Inner Ear'. *Neuroscience Letters* 534 (February):101–6. https://doi.org/10.1016/j.neulet.2012.11.018.

Zhao, H.-B., T. Kikuchi, A. Ngezahayo, and T. W. White. 2006. 'Gap Junctions and Cochlear Homeostasis'. *The Journal of Membrane Biology* 209 (2–3): 177–86. https://doi.org/10.1007/s00232-005-0832-x.

Zhao, Tong, Xiuzhen Liu, Zehua Sun, Jinjin Zhang, Xiaolin Zhang, Chaoyun Wang, Ruishuang Geng, Tihua Zheng, Bo Li, and Qing Yin Zheng. 2020. 'RNA-Seq Analysis of Potential lncRNAs for Age-Related Hearing Loss in a Mouse Model'. *Aging* 12 (8): 7491–7510. https://doi.org/10.18632/aging.103103.

Zheng, J., W. Shen, D. Z. He, K. B. Long, L. D. Madison, and P. Dallos. 2000. 'Prestin Is the Motor Protein of Cochlear Outer Hair Cells'. *Nature* 405 (6783): 149–55. https://doi.org/10.1038/35012009.